

OROBOROS INSTRUMENTS  
high-resolution respirometry

Mitochondrial Physiology Network



# Mitochondrial Pathways and Respiratory Control

## An Introduction to OXPHOS Analysis

Erich Gnaiger

Mitochondr Physiol Network 17.18

OROBOROS MiPNet Publications 2012



# Mitochondrial Pathways and Respiratory Control

## An Introduction to OXPHOS Analysis

**Erich Gnaiger**

Mitochondr Physiol Network 17.18

OROBOROS MiPNet Publications 2012

©2012 OROBOROS INSTRUMENTS GmbH, Innsbruck, Austria  
Printed by Steiger Druck GmbH, Axams, Austria. [steigerdruck@tirol.com](mailto:steigerdruck@tirol.com)

**3<sup>rd</sup> edition: 2400 prints**

**ISBN 978-3-9502399-6-6**

1<sup>st</sup> edition (2007): 1000 prints; electronic 1<sup>st</sup> edition, ISBN 978-3-9502399-0-4

Open Access: [www.bioblast.at/index.php/Gnaiger\\_2012\\_MitoPathways](http://www.bioblast.at/index.php/Gnaiger_2012_MitoPathways)

OROBOROS INSTRUMENTS Corp.  
high-resolution respirometry  
Schöpfstr. 18  
A-6020 Innsbruck, Austria  
[erich.gnaiger@oroboros.at](mailto:erich.gnaiger@oroboros.at)  
[www.oroboros.at](http://www.oroboros.at)    [www.bioblast.at](http://www.bioblast.at)

D. Swarovski Research Lab.  
Dept. Visceral, Transplant and  
Thoracic Surgery  
Medical University of Innsbruck  
A-6020 Innsbruck, Austria  
[www.bioblast.at/index.php/MitoCom](http://www.bioblast.at/index.php/MitoCom)

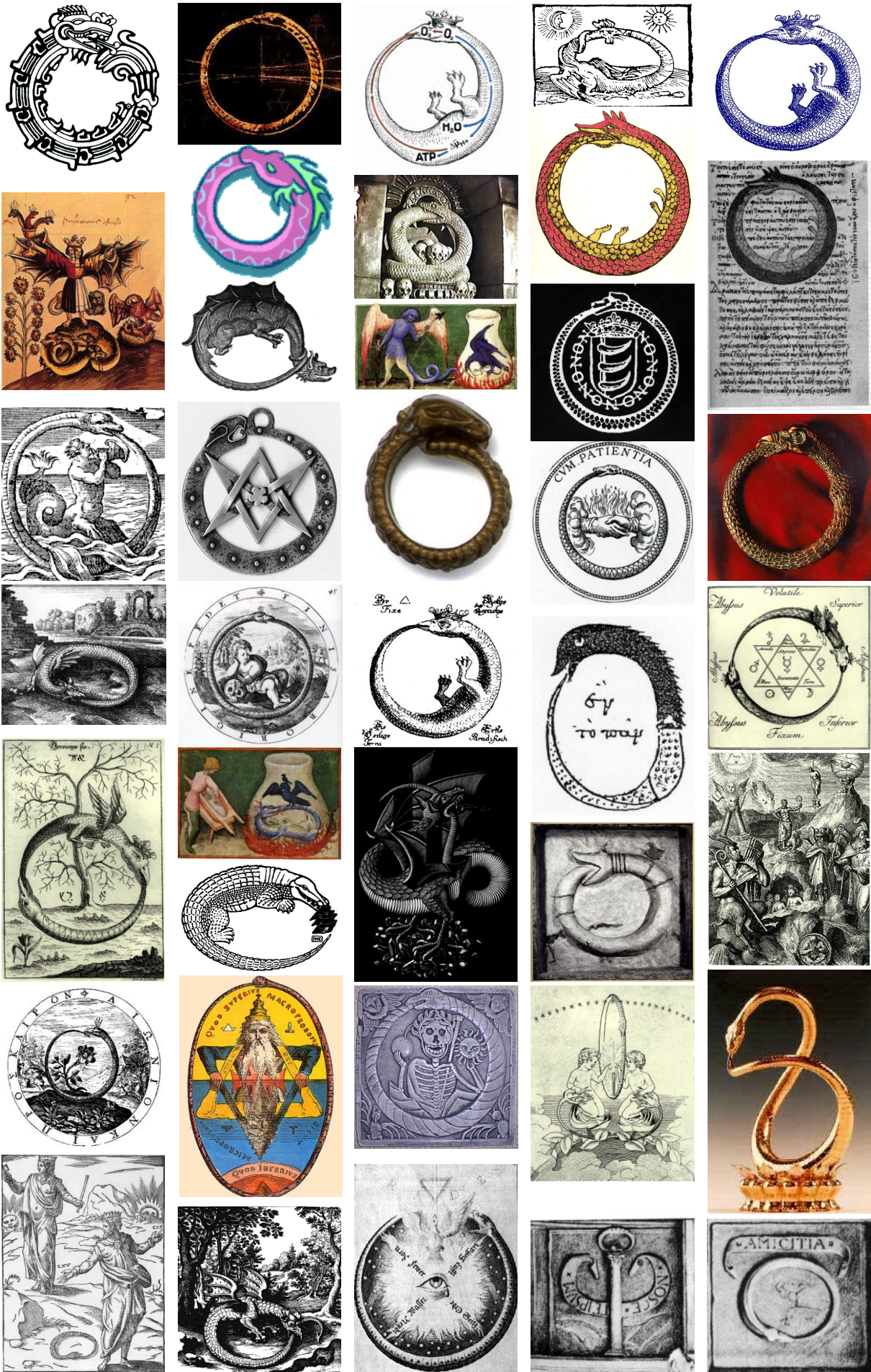




Fig. 1. The Blue Book: Mitochondrial Pathways and Respiratory Control 1<sup>st</sup> edition (2007). 1<sup>st</sup> Mitochondrial Physiology Summer School, MiPsummer July 2007, Schröcken, Austria.

# Mitochondrial Pathways and Respiratory Control

## Preface

The present introduction to the analysis of oxidative phosphorylation (OXPHOS analysis) combines concepts of bioenergetics and biochemical pathways related to mitochondrial core energy metabolism. This provides the basis for the design of substrate-uncoupler-inhibitor titration (SUIT) protocols in novel O2k-assays established since publication in 2007 of 'Mitochondrial Pathways' (The Blue Book, 1<sup>st</sup> ed; Fig. 1).

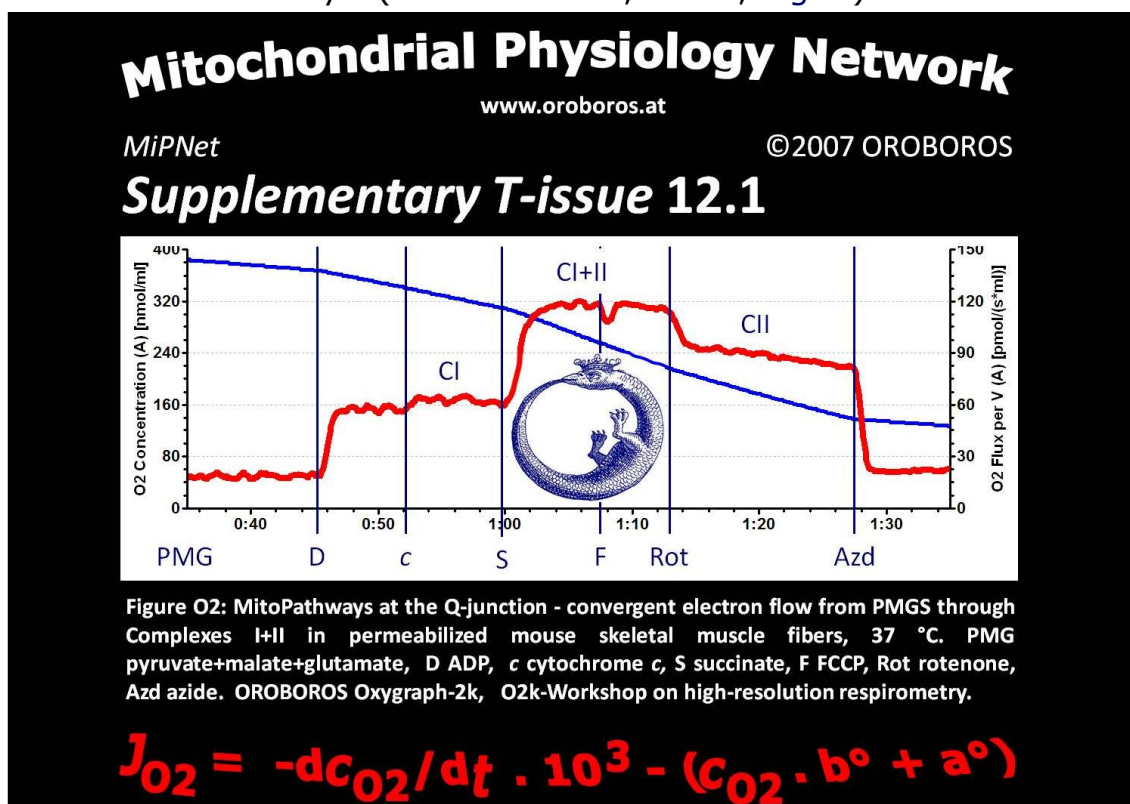


Fig. 2. OROBOROS INSTRUMENTS presented results not merely as a **Paper** but as a supplementary **T-issue** printed on the OROBOROS **T-shirt**. OXPHOS analysis in an O2k-experiment 2007-04-14 AB-03 performed at an O2k-Workshop on HRR (IOC39, April 2007, Schröcken, Vorarlberg, Austria).



Application of SUIIT protocols for OXPHOS analysis is a component of metabolic phenotyping (Fig. 2). OXPHOS analysis extends conventional bioenergetics to the level of mitochondrial physiology for functional diagnosis in health and disease. SUIIT protocols with substrate combinations are now established in studies with isolated mitochondria, permeabilized cells and permeabilized muscle fibres and tissue homogenates using high-resolution respirometry (HRR). The OROBOROS Oxygraph-2k (O2k) represents a unique instrument for HRR. No other platform is suited for application of SUIIT protocols due to a restricted number of serial titrations available in multiwell systems or insufficient signal stability and restricted oxygen capacity in small chambers.

A *Mitochondrial Physiology Network* has evolved as (i) a network of scientists linked by applications of the O2k (WorldWide MiPNet: [www.orooboros.at/?MiPNet](http://www.orooboros.at/?MiPNet)), and (ii) a format of publications available on the OROBOROS website, which summarizes protocols, introductory guidelines and discussions of concepts (MiPNet Protocols: [www.orooboros.at/?O2k-Protocols](http://www.orooboros.at/?O2k-Protocols)). (iii) Beyond the restricted space for references selected in the printed edition, O2k-Publications are listed as supplementary information that is updated continuously on the Bioblast wiki ([www.bioblast.at/index.php/O2k-Publications](http://www.bioblast.at/index.php/O2k-Publications)). The number of O2k-Publications increases rapidly (presently >800) with extending areas of biomedical and clinical applications of the OROBOROS Oxygraph-2k. (iv) A glossary is presented on the Bioblast 'MitoPedia' website with emphasis on developing a consistent terminology in mitochondrial physiology ([www.bioblast.at/index.php/MitoPedia Glossary: Terms and abbreviations](http://www.bioblast.at/index.php/MitoPedia_Glossary:_Terms_and_abbreviations)).

'MitoPathways' has become an element of high-resolution respirometry and mitochondrial physiology. A mosaic evolves by combining the elements into a picture of modern mitochondrial respiratory physiology.

I thank all contributors to the *Mitochondrial Physiology Network* for their cooperation and feedback. In particular, I want to acknowledge the experimental contributions by the authors and co-authors of various publications emerging from international cooperations. Without the team of OROBOROS INSTRUMENTS, including the partners in electromechanical engineering (Oxygraph-2k; Philipp Gradl, WGT Elektronik, Kolsass, Austria) and software development (DatLab; Lukas Gradl, software security networks, Innsbruck, Austria) the experimental advances on 'MitoPathways' would not have been possible.

For references and notes see Bioblast online information:



[www.bioblast.at/index.php/Gnaiger\\_2012\\_MitoPathways](http://www.bioblast.at/index.php/Gnaiger_2012_MitoPathways)

Erich Gnaiger  
Innsbruck, July 2007 - Dec 02 2012





## Contents

<b>1. OXPHOS Analysis</b> .....	7
<b>2. MitoPathways to Complex I.</b> Respiratory Substrate Control with Pyruvate, Malate and Glutamate	19
<b>3. MitoPathways to Complex II,</b> Glycerophosphate Dehydrogenase and ETF .....	26
<b>4. MitoPathways to Complexes I+II.</b> Convergent Electron Transfer at the Q-junction .....	29
<b>5. Respiratory States,</b> Coupling Control and Coupling Control Ratios .....	44
<b>6. Conversions of Metabolic Fluxes</b> .....	51
<b>A1. Respiratory Coupling States and Coupling Control Ratios</b> .....	54
<b>A2. Substrates, Uncouplers and Inhibitors</b> .....	56
<b>References</b> .....	59
<a href="http://www.bioblast.at/index.php/Gnaiger_2012_MitoPathways">www.bioblast.at/index.php/Gnaiger_2012_MitoPathways</a>	
<b>Bioblast Wiki</b> .....	61
<b>The OROBOROS</b> - Feeding on Negative Entropy .....	63



Mitochondrial Oroboros by Odra Noel

Cover: Suspended human umbilical vein endothelial cells by Gunde Rieger



## Support: K-Regio Project *MitoCom Tyrol*

The aim of the project is the development, evaluation and application of a new high-resolution instrument, the O2k-Fluorometer, which builds upon the OROBOROS Oxygraph-2k developed and extended since 2001 by OROBOROS INSTRUMENTS and WGT-Elektronik. The Oxygraph-2k (O2k) provides the instrumental basis for high-resolution respirometry (HRR) and represents world-wide the technologically leading instrument for diagnostic evaluation of mitochondrial respiratory function, presently represented in 37 countries.

The integration of fluorometry and spectrophotometry into the O2k opens up the potential for the analysis of various diagnostically significant cellular functions, simultaneously with the measurement of mitochondrial respiration. In particular, HRR is now combined with new modules for the fluorometric detection of reactive oxygen species (ROS; oxidative stress) and mitochondrial membrane potential using established fluorescent dyes. This innovation further establishes the technological leadership and sole-source status of the O2k as a high-end diagnostic instrument.

The new edition of 'Mitochondrial Pathways' explains the conceptual basis of established protocols for the study of respiratory control, and for the design and optimization of new experimental protocols to support innovative applications of HRR at an advanced level of OXPHOS analysis.

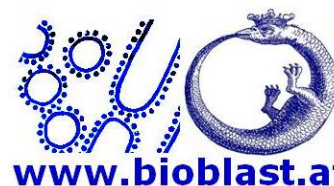


Contribution to K-Regio project *MitoCom Tyrol*, funded in part by the Tyrolian Government and the European Regional Development Fund (ERDF).



## Citation

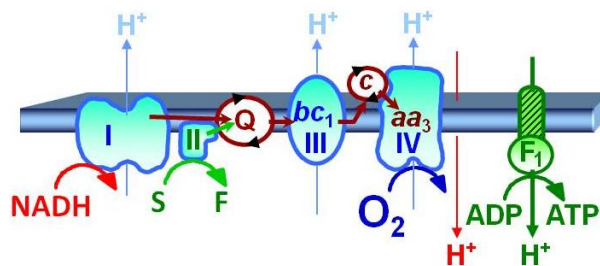
Gnaiger E (2012) Mitochondrial Pathways and Respiratory Control. An Introduction to OXPHOS Analysis. Mitochondr Physiol Network 17.18. OROBOROS MiPNet Publications, Innsbruck: 64 pp.



References: [www.bioblast.at/index.php/Gnaiger\\_2012\\_MitoPathways](http://www.bioblast.at/index.php/Gnaiger_2012_MitoPathways)




## Chapter 1. OXPHOS Analysis



*The protoplasm is a colony of bioblasts. Microorganisms and granula are at an equivalent level and represent elementary organisms, which are found wherever living forces are acting, thus we want to describe them by the common term bioblasts.*

Richard Altmann (1894)

Section		Page
	1. Chemiosmotic Coupling.....	7
	2. From Oxygen Concentration to Oxygen Flux .....	8
	3. Metabolic Forces .....	11
	4. Fluxes and Forces: Coupling and Efficiency .....	13
	5. Electron Gating .....	14
	6. Electron Transfer: Q-Junction .....	15
	7. Biochemical Thresholds and the Q-Junction....	16
	8. Boundary Conditions .....	16

Oxidative phosphorylation (OXPHOS) is a key element of bioenergetics, extensively studied to resolve the mechanisms of energy transduction in the mitochondrial electron transfer system and analyze various modes of mitochondrial (mt) respiratory control in health and disease. OXPHOS flux control is exerted by (i) coupling of electron transfer to proton translocation and ATP synthesis mediated by the chemiosmotic, proton motive force, and uncoupling by proton leaks; (ii) substrates and catalytic capacities of respiratory complexes, carriers, transporters, and mt-matrix enzymes of core energy metabolism; (iii) kinetic regulation by concentrations of ADP, inorganic phosphate, oxygen and reduced substrates feeding electrons into the electron transfer system; (iv) specific inhibitors such as NO and H<sub>2</sub>S.

### 1. Chemiosmotic Coupling

Peter Mitchell's chemiosmotic coupling theory explains the fundamental mechanism of mitochondrial and microbial energy transformation, marking Richard Altmann's 'bioblasts' as the systematic unit of bioenergetics and of the human symbiotic 'supraorganism' with microbial-mammalian co-metabolic pathways. The transmembrane chemiosmotic force or electrochemical proton potential,  $\Delta p$ , has a chemical component (proton gradient) and electrical component (membrane potential).  $\Delta p$  provides the link between electron transfer and phosphorylation of ADP to ATP (Fig. 1.1).



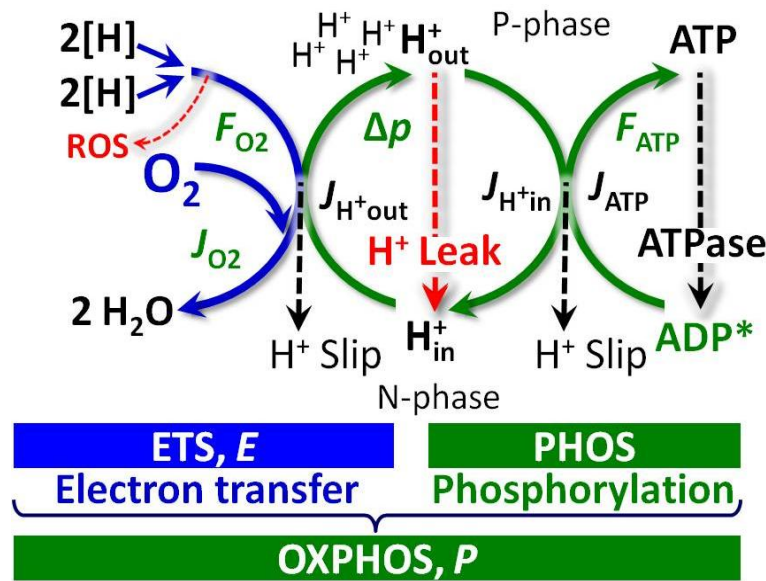


**Fig. 1.1. Energy transformation** in coupled fluxes,  $J$ , and forces,  $F$  and  $\Delta p$ , of oxidative phosphorylation.  $2[H]$  indicates the reduced hydrogen equivalents of CHO substrates and electron transfer to oxygen.  $J_{H^+out}$  is coupled output flux. Proton leaks dissipate energy of translocated protons from low pH in the positive P-phase to the negative N-phase.

Mitochondrial respiration is the exergonic input tightly but not fully coupled to the endergonic output of phosphorylation. OXPPOS capacity ( $P$ ) is measured at saturating ADP concentration ( $ADP^*$ , Fig. 1.1), which cannot be tested in living cells. ETS capacity ( $E$ ) is quantified by uncoupler (protonophore) titrations to obtain maximum flux in mitochondrial preparations or living cells (Fig. 1.2).  $E$  and  $P$  are numerically identical only if the phosphorylation system (adenylate nucleotide translocase, phosphate carrier, ATP synthase) does not exert control over coupled respiration. A shift towards control of OXPPOS by the phosphorylation system is observed when ETS capacity is increased by the additive effect of convergent electron input into the Q-junction.

## 2. From Oxygen Concentration to Oxygen Flux

OXPPOS analysis uses respirometry as a fundamental approach to study oxygen consumption as an element of mitochondrial function in aerobic core metabolism. Oxygen flux times the driving force of the oxidation reaction provide the input power into the OXPPOS system. In a closed oxygraph chamber, the oxygen concentration declines over time as a result of respiratory processes. The time derivative, therefore, is a negative number. Why is then the 'rate of oxygen consumption' not expressed as a negative value? Why is the term 'oxygen flux' used in this context of chemical reactions? The rationale is based on fundamental concepts of physical chemistry and the thermodynamics of irreversible processes in open and closed systems (Gnaiger 1993).

Concentration,  $c_B$  [ $\text{mol}\cdot\text{dm}^{-3}$ ], is the amount of substance,  $n_B$  [ $\text{mol}$ ], per unit of volume,  $V$ . The amount of elemental oxygen dissolved per volume of aqueous medium in the Oxygraph chamber is the oxygen concentration,  $c_{O_2}$ , measured by the polarographic oxygen sensor as an electric current,  $I$  [ $\text{A}$ ], and converted into a voltage [ $\text{V}$ ]. At any time  $t$  [ $\text{s}$ ], this raw signal is calibrated to record oxygen concentration  $c_{O_2,t}$  (Fig. 1.2). For units of oxygen concentration, see Chapter 6.2.

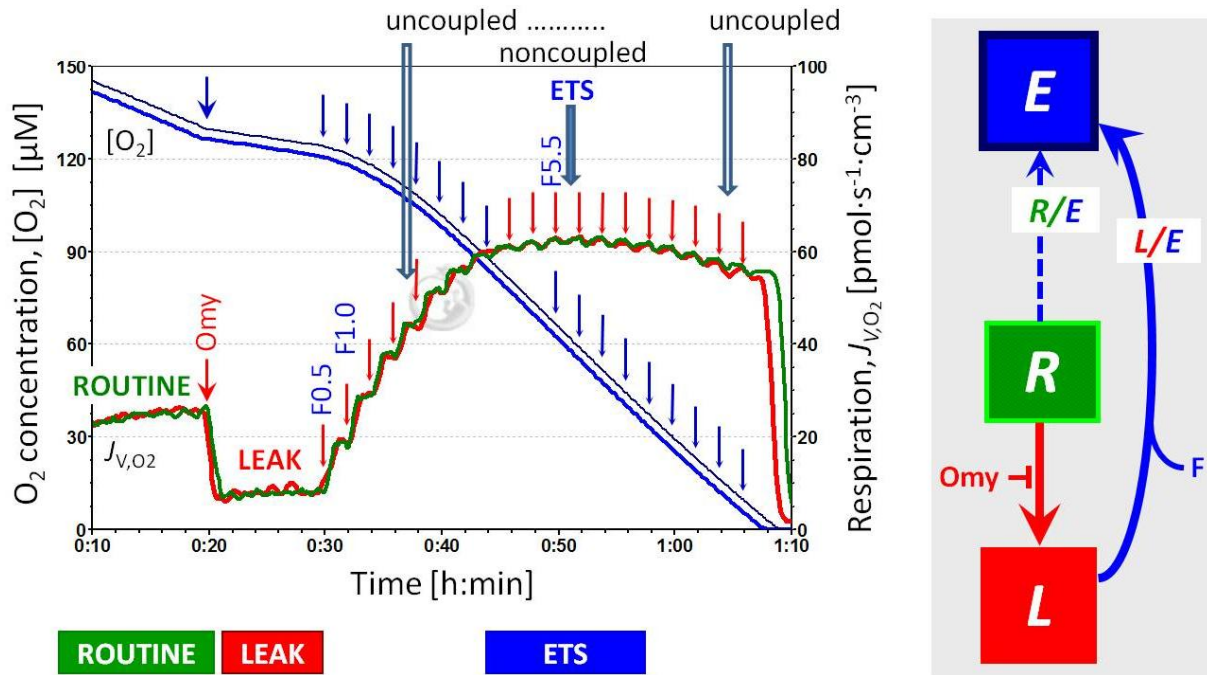


**Fig. 1.2. Oxygen concentration and oxygen flux in intact cells with coupling control protocol.** High-resolution respirometry (OROBOROS Oxygraph-2k with TIP2k) with parental hematopoietic 32D cells at  $1.1 \cdot 10^6$  cells/cm<sup>3</sup> suspended in culture medium RPMI at 37 °C. Replicate measurements in the two O2k-chambers (2 cm<sup>3</sup>). Superimposed plots of oxygen concentration [O<sub>2</sub>] and volume-specific oxygen flux,  $J_{v,O_2}$ , calculated as the negative time derivative of oxygen concentration. ROUTINE respiration (R) is followed by inhibition of ATP synthase (manual titration of oligomycin, 2 μg·ml<sup>-1</sup>) to induce the nonphosphorylating LEAK state (L). Automatic titration of uncoupler (10 mM FCCP in the TIP2k) in steps of 0.1 μl corresponding to a step increase in the final concentration of 0.5 μM FCCP at intervals of 120 s. Maximum noncoupled flux (capacity of the electron transfer system, ETS; state E) is reached at 5.5 μM FCCP. The L/E ratio is 0.10. Respiration is inhibited at higher [FCCP], unrelated to sample dilution (<1%). O2k-experiment 2005-04-09 EF-03, carried out by participants of an O2k-Workshop. Modified after Gnaiger (2008).

The oxygen concentration in pure water at equilibrium with air at standard barometric pressure of 100 kPa is 254.8 to 207.3 μmol/litre in the range of 25 °C to 37 °C. In the 'open' Oxgraph chamber, in which the aqueous medium is in equilibrium with a gas phase (such as air), the partial oxygen pressure,  $p_{O_2}$  [kPa] is identical in the gas phase and aqueous phase. The oxygen concentration, however, is very different in air and water. At equilibrium, the gas concentration in the gas phase is much higher than in aqueous solution. The dissolved oxygen concentration is proportional to the partial oxygen pressure at constant temperature and composition of the aqueous medium. This proportionality constant is the oxygen solubility,  $S_{O_2}$  [μM/kPa]. In pure water at 25 °C (37 °C), the oxygen solubility is 12.56 (10.56) μM/kPa, but reduced by a factor of 0.89 to 0.92 in various culture and respiration media (0.92 for MiR06).



Cell respiration is an exergonic process by which reduced substrates (CHO) are oxidised internally and molecular oxygen (or another external electron acceptor) is consumed in exchange with the environment. In the 'closed' Oxygraph chamber, which is sealed against any exchange of oxygen across the chamber walls and sealings, all oxygen consuming reactions cause the oxygen concentration to decline with time. If oxygen consumption is activated, then oxygen concentration falls off more steeply (Fig. 1.2). Oxygen concentration remains constant over time and the slope is zero when all processes reacting with oxygen are fully inhibited.

A linear negative slope, i.e. a constant drop of oxygen concentration with time in the closed Oxygraph chamber, is the result of a constant rate of the chemical reaction. Defining the reaction as



then the oxygen consumption rate per unit volume (= oxygen flux, volume-specific) is proportional to the negative slope of oxygen concentration with time. Take the difference of oxygen concentration (left Y-axis) between two time points (X-axis in Fig. 1.2),

$$\text{Concentration axis: } \Delta c_{\text{O}_2} = c_{\text{O}_2,2} - c_{\text{O}_2,1} \quad (1.2a)$$

$$\text{Time axis: } \Delta t = t_2 - t_1 \quad (1.2b)$$

The slope between these points is the rate of concentration change,

$$r_{\text{O}_2} = \Delta c_{\text{O}_2} / \Delta t \quad (1.3)$$

Metabolic flux (reaction 1.1), however, is the *negative* slope (see Eq. 1.5),

$$J_{V,\text{O}_2} = -(\Delta c_{\text{O}_2} / \Delta t) \quad (1.4)$$

In differential form ( $dt$  = infinitesimally small  $\Delta t$ ), the expression becomes

$$\text{Closed system: } J_{V,\text{O}_2} = -(dc_{\text{O}_2} / dt) \quad (1.5a)$$

$$\text{General: } J_{V,\text{O}_2} = d_r n_{\text{O}_2} / dt \cdot v_{\text{O}_2}^{-1} \cdot V^{-1} = d_r \xi_{\text{O}_2} / dt \cdot V^{-1} \quad (1.5b)$$

With the differential form (Eq. 1.5), gradual changes of oxygen flux can be evaluated (Fig. 1.2), in contrast to the assumption of linearity in the difference form of Eq. 1.4. Generalization from closed to open systems is achieved by the concept of *advancement* of reaction,  $d_r \xi_{\text{O}_2} = d_r n_{\text{O}_2} \cdot v_{\text{O}_2}^{-1}$ . The subscript  $\text{O}_2$  in  $d_r \xi_{\text{O}_2}$  indicates that the stoichiometric number of oxygen in reaction 1.1 is taken as unity ( $v_{\text{O}_2} = -1$ ). Hence respiratory flux,  $J_{\text{O}_2}$ , refers to a stoichiometric form of oxygen-consuming reactions where 1 mol of  $\text{O}_2$  is transformed. The negative sign in  $v_{\text{O}_2}$  yields  $J_{\text{O}_2}$  with a positive value.

*Volume-specific* oxygen flux,  $J_{V,\text{O}_2}$  (Eq. 1.5; Fig. 1.2), in cell respiration is a quantitative measure of the internal reaction per volume of the experimental chamber. Dividing  $J_{V,\text{O}_2}$  [ $\text{pmol} \cdot \text{s}^{-1} \cdot \text{ml}^{-1}$ ] by cell concentration (number of cells per volume [ $10^6 \cdot \text{ml}^{-1}$ ]) converts volume-specific oxygen flux to *system-specific* oxygen flow,  $I_{\text{O}_2}$  [ $\text{pmol} \cdot \text{s}^{-1} \cdot 10^{-6}$  cells]. The cell (or  $10^6$  cells) is a *system*. Oxygen flow is an *extensive*



quantity that changes with the size of the system (Fig. 1.3). A *specific* quantity is obtained when the extensive quantity is divided by *system size*. *Cell-mass specific* oxygen flux,  $J_{O_2}$  [ $\text{pmol}\cdot\text{s}^{-1}\cdot\text{mg}^{-1}$ ], is flow per cell,  $I_{O_2}$  [ $\text{pmol}\cdot\text{s}^{-1}\cdot 10^{-6}$  cells], divided by mass per cell [ $\text{mg}\cdot 10^{-6}$  cells]; or volume-specific flux,  $J_{V,O_2}$  [ $\text{pmol}\cdot\text{s}^{-1}\cdot\text{ml}^{-1}$ ], divided by mass per volume [ $\text{mg}\cdot\text{ml}^{-1}$ ]. Mitochondrial (mt) markers are determined for expressing mt-content in cells or tissues and oxygen flux in terms of a mt-marker (Fig. 1.3). Commonly used mt-markers are activities of citrate synthase (mt-matrix marker) and cytochrome c oxidase (inner mt-membrane marker). Flux control ratios are based on a functional mt-marker (Pesta et al 2011).

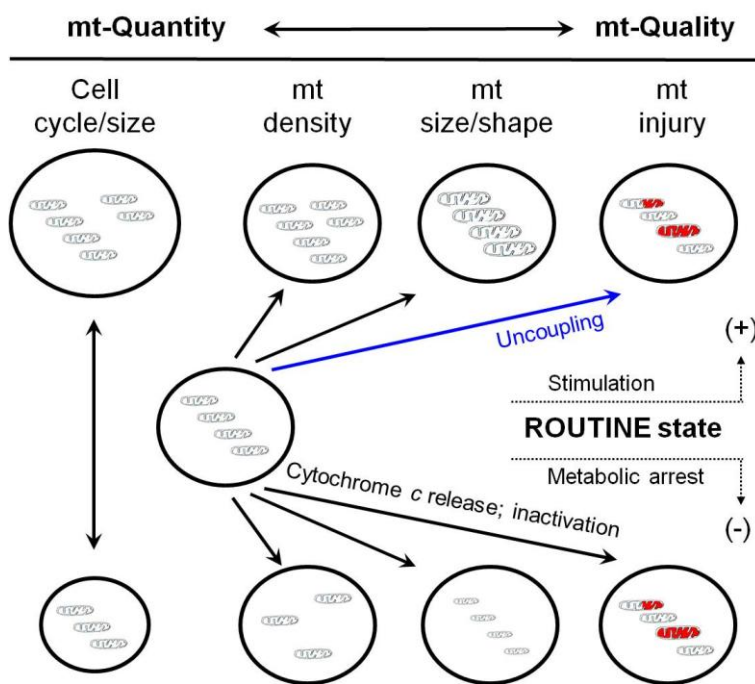


**Fig. 1.3. Oxygen flow (per cell), cell-specific oxygen flux (per cell size), or mt-specific oxygen flux (per mitochondrial marker).** ROUTINE respiration of intact cells is a function of metabolic state. Oxygen flow per million cells,  $I_{O_2}$  [ $\text{pmol}\cdot\text{s}^{-1}\cdot 10^{-6}$  cells] depends on cell size, mt-density and mt-quality. These factors are separated when flux is normalized for cell size or mt-content. Modified after Renner et al (2003).

### 3. Metabolic Forces: Electric and Chemical Potentials

Power is energy per time, integrating flows and forces, the basis for efficiency or irreversible entropy production. Flow times force yields power. For the chemical reaction,  $r$  (Eq. 1.5b),

$$\text{Flow times force: } P_r = I_{O_2} \cdot F_{O_2,r} \quad I_{O_2} = d_r \xi_{O_2} / dt = d_r n_{O_2} / dt \cdot v_{O_2}^{-1} \quad (1.6a)$$

$$\text{Flux times force: } P_{V,r} = J_{V,O_2} \cdot F_{O_2,r} \quad J_{V,O_2} = d_r \xi_{O_2} / dt \cdot V^{-1} \quad (1.6b)$$

Electric power is flow or current ( $I_{el}$ ; units ampere [ $A=C\cdot s^{-1}$ ]) times force or electric potential difference ( $F_{el}$ ; units volt [ $V=J\cdot C^{-1}$ ]) where electric charge is expressed in coulombs [C].

$$\text{Electric, el: } P_{el} = I_{el} \cdot F_{el} \quad F_{el} = \partial G / \partial_{el} \xi \quad [J\cdot C^{-1}] \quad (1.7a)$$

$$\text{Displacement, d: } P_d = I_{B,d} \cdot F_{B,d} \quad F_{B,d} = \partial G / \partial_d \xi_B \quad [J\cdot \text{mol}^{-1}] \quad (1.7b)$$

$$\text{Reaction, r: } P_r = I_{B,r} \cdot F_{B,r} \quad F_{B,r} = \partial G / \partial_r \xi_B \quad [J\cdot \text{mol}^{-1}] \quad (1.7c)$$



The power of a transformation,  $P_{tr}$ , is the Gibbs energy change per time,  $P_{tr}=d_{tr}G/dt$  [ $W=J\cdot s^{-1}$ ]. The total Gibbs energy change,  $dG$ , is the sum of all partial energy transformations ( $dG = \sum d_{tr}G = d_{el}G + d_dG + d_rG + ..$ ), which is a concept of eminent importance in the chemiosmotic theory. Gibbs energy change,  $dG$ , measured over a prolonged period of time,  $\Delta t$ , becomes an energy change of  $\Delta G$  (compare Eq. 1.4 and 1.5).

A glorious didactic pitfall in most famous textbooks of biochemistry and bioenergetics is the confusing presentation of  $\Delta G$ , propagating a mix-up of energy change [J] and driving force of chemical reactions [ $J\cdot mol^{-1}$ ]. The generalized scalar forces in thermodynamics are partial changes (derivatives) of Gibbs energy per advancement,  $F_{tr} = \partial G/\partial_{tr}\xi$  (Eq. 1.7). These ergodynamic forces are potential differences (Gnaiger 1993). The chemiosmotic potential or protonmotive force,  $\Delta p$ , is the sum of the partial electric and chemical (osmotic) forces of proton translocation across a membrane. The redox potential difference expresses force on the basis of electric charge [ $J\cdot C^{-1}=V$ ]. The chemical potential difference,  $\Delta\mu_B$ , expresses chemical force on the basis of *amount of substance* [ $J\cdot mol^{-1}=Jol$ ]. Unfortunately, the unit 'Jol' – or any term denoting a unit for chemical force - does not exist; it should be coined in analogy to the unit volt, facilitating the conceptual distinction between Gibbs energy change [J] and Gibbs force [ $Jol=J\cdot mol^{-1}$ ]. Logically, a *force* cannot be an *energy* difference,  $\Delta G$  [J]. A voltage [V] is not electric energy [J]. Gibbs force is a chemical potential difference,  $\sum\mu_i\cdot\nu_i$ , which can be converted to an electric potential difference by multiplication with the number of charges and the Farady constant,  $F= 96\,485.3\ C\cdot mol^{-1}$  or  $F= 0.0964853\ kJ\cdot mol^{-1}/mV$ .

Flows are advancement per time,  $I_{tr} = d_{tr}\xi/dt = d_{tr}X_i/dt \cdot \nu_i^{-1}$  (Eq. 1.5b).  $X_i$  is the generalized property (*transformant*) involved in a transformation, tr.  $X_i(el)$  is charge expressed in coulombs [C].  $X_i(d, r)$  is amount of displaced or reacting substance expressed in moles [mol] (Eq. 1.7).

Electric force,  $F_{el}$  [V], is an *electric potential difference*, giving rise to the term mitochondrial *membrane potential*,  $\Delta\psi$ . The partial chemical force of proton transduction or dislocation,  $d$ , is the *chemical potential difference*,  $\Delta\mu_{H^+}$  [ $kJ\cdot mol^{-1}$ ], which is a function of the proton activity,  $a_{H^+}$  [ $mol\cdot dm^{-3}$ ], or pH at phases  $i$ ,

$$\text{Potential:} \quad \mu_{H^+,i} = -RT\cdot\ln a_{H^+,i} = -RT\cdot\ln(10)\cdot pH_i \quad (1.8a)$$

$$\text{Potential difference:} \quad \Delta\mu_{H^+} = -RT\cdot\ln(10)\cdot\Delta pH = -2.3\cdot RT\cdot(pH_2-pH_1) \quad (1.8b)$$

Choosing  $i=1$  as the negative N-phase ( $\nu_{H^+,1}=-1$ ) and  $i=2$  as the positive P-phase ( $\nu_{H^+,2}=1$ ) defines the direction of translocation against the electrochemical gradient. At 25 °C or 37 °C, a difference of -1 pH yields  $\Delta\mu_{H^+} = 5.7$  or  $5.9\ kJ\cdot mol^{-1}$ , equivalent to 59.2 or 61.5 mV (Chapter 6.3).

Force, energy and power are positive when conserving work by pumping protons uphill from high to low pH (Fig. 1.1). Output power requires coupling to input power (Fig. 1.1). Input force, energy and power



have a negative sign, indicating the spontaneous downward or dissipative direction of energy transformation, consistent with entropy production of irreversible processes. Thus irreversible thermodynamics provides the conceptual framework to describe all partial, simultaneous fluxes and forces in a consistent format of the dissipation function (Prigogine 1967). This unifies the description of chemical and electrochemical energy transformations, achieving a simplification compared to the divergent symbols and sign conventions in classical descriptions (Gnaiger 1993).

Experimental OXPHOS analysis has the potential to combine measurement of flows by HRR (electron transfer quantified by oxygen flow as input, ATP flow as output) and forces, such as the mitochondrial membrane potential,  $\Delta\psi$ , in an O2k-MultiSensor System using either potentiometric or fluorometric signals to study the equilibrium distribution of ions across the inner mt-membrane. The chemical  $\Delta p$  component of the protonmotive force must be determined separately, or is diminished by incubation conditions including a high inorganic phosphate concentration. A shortcircuit ( $H^+$  leak) dissipates the energy of the translocated protons, which otherwise is used to phosphorylate ADP to ATP, with an output force of 52 to 66 kJ/mol ATP under intracellular conditions. The efficiency of coupling is diminished further by potential proton slips of the proton-energy conserving pumps (Complexes CI, CIII and CIV). Whereas the proton leak depends on  $\Delta p$  and is a property of the inner membrane including the boundaries between membrane-spanning proteins and the lipid phase, proton slip is a property of the proton pumps when the proton slips back to the matrix side within the proton pumping process and is thus mainly dependent on flux. Production of reactive oxygen species (ROS) is another component reducing the coupling between oxygen flux and ATP turnover.

#### 4. Fluxes and Forces: Coupling and Efficiency

The flux ratio between ATP production,  $J_{ATP}$ , and oxygen consumption,  $J_{O_2}$ , is the P/O<sub>2</sub> ratio (or P/O ratio with atomic oxygen as a reference). This is frequently referred to as the 'coupling efficiency', with focus on metabolic fluxes in OXPHOS analysis. Coupling efficiency is quantified by the simultaneous determination of input and output fluxes, e.g. by measurement of oxygen flux and ATP flux in the O2k-MultiSensor System, using the O2k-Fluorescence LED2-Module with Mg-green.

An indirect estimate of coupling efficiency is obtained by sequential measurement of LEAK respiration and ETS capacity, which can be obtained in intact cells (Fig. 1.2). The L/E coupling control ratio provides an estimate of the actual coupling efficiency relative to the upper limit of stoichiometric coupling in a tightly or mechanistically coupled system. LEAK respiration is the LEAK oxygen flux,  $L$ , compensating for proton leak, slip and cation cycling, with ROS production usually playing a minor role (Fig. 1.1). LEAK respiration is measured as mitochondrial respiration in



the LEAK state, in the presence of reducing substrate(s), but absence of ADP, or after inhibition of the phosphorylation system (oligomycin or atractyloside; Fig. 1.2). In this non-phosphorylating resting state, the electrochemical proton gradient is increased to a maximum, exerting feedback control by depressing oxygen flux to a level determined by the proton leak and the  $H^+/O_2$  ratio ( $H^+/O$  ratio). In this state of maximum protonmotive force, LEAK respiration is higher than the LEAK component in ADP-stimulated respiration (OXPHOS capacity). OXPHOS capacity cannot be determined in intact cells.

Respiratory control ratios and coupling control ratios need to be combined for proper evaluation of OXPHOS coupling efficiency. Ergodynamic efficiencies, in turn, require the combined information on coupling efficiency and force ratios, including evaluation of redox potentials, chemiosmotic potentials and phosphorylation potentials (Gibbs forces). Efficiency is well defined in thermodynamics based on the entropy law, as an output/input power ratio with a maximum of 1.0. Specific metabolic power [ $J \cdot s^{-1} \cdot g^{-1} = W \cdot g^{-1}$ ] is not identical to metabolic flux [ $mol \cdot s^{-1} \cdot g^{-1}$ ]. Classical thermodynamics considers efficiency as a ratio of work output and heat or enthalpy input (caloric input, the heat engine).

Efficiency in the thermodynamics of irreversible processes takes into account fluxes and forces (specific power = flux times force). Efficiency (ergodynamic efficiency) is the product of coupling efficiency (flux ratio) and a conjugated force ratio. From Fig. 1.1, calculation of ergodynamic OXPHOS efficiency requires simultaneous measurement of input oxygen flux and force ( $J_{O_2} \cdot F_{O_2}$ ) and output ATP flux and force ( $J_{ATP} \cdot F_{ATP}$ ). The Gibbs force of oxygen consumption,  $F_{O_2}$ , is typically  $-450$  kJ/mol  $O_2$ . Efficiency is then calculated as  $-(J_{ATP} \cdot F_{ATP}) / (J_{O_2} \cdot F_{O_2})$ . Maximum efficiency can be obtained only by compromising speed and slowing down when approaching equilibrium, whereas maximum power is achieved at the cost of energy required for fast but less efficient processes (Fig. 1.4).

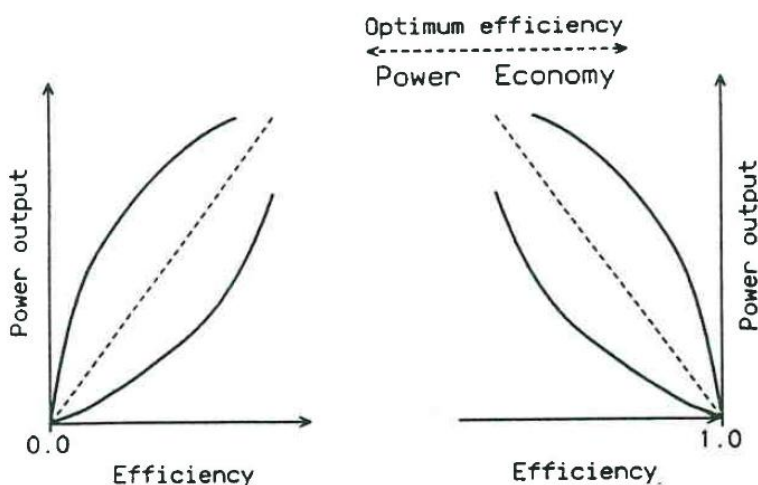


**Fig. 1.4. Optimum efficiency** depends on the strategy of either maximizing output power or efficiency. From Gnaiger E (1993) Efficiency and power strategies under hypoxia. Is low efficiency at high glycolytic ATP production a paradox? In: *Surviving Hypoxia: Mechanisms of Control and Adaptation*. Hochachka et al eds. CRC Press, Boca Raton, Ann Arbor, London, Tokyo: 77-109.



## 5. Electron Gating

Electrons flow to oxygen along linear thermodynamic cascades (electron transfer chains) from either Complex I with three coupling sites, from Complex II with two coupling sites, or from other respiratory complexes which do not have a roman number. The CI- and CII-pathways of electron transfer are conventionally separated by using either NADH-linked substrates, such as pyruvate+malate, or the classical succinate+rotenone combination, to analyze site-specific  $H^+/O$  and  $P/O$  ratios or defects of specific respiratory complexes in functional diagnosis. Electron gating is the experimental separation of various electron transfer pathways converging at the Q-junction (Fig. 1.5). Even without having been properly recognized and defined by a name, electron gating is common to the extent of establishing a bioenergetic paradigm in studies of OXPHOS with isolated mitochondria or permeabilized cells.

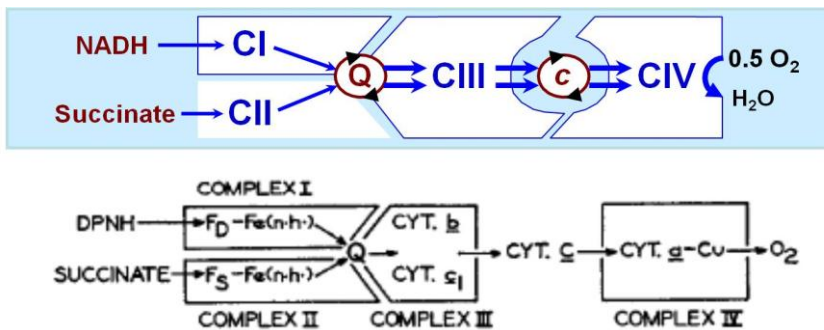


FIG. 5. Schematic representation of the four functional primary complexes and their sequential arrangement in the electron transfer system.  $F_D$ , DPNH dehydrogenase flavoprotein;  $F_S$ , succinic dehydrogenase flavoprotein.

**Fig. 1.5. Convergent CI+II-linked electron flow at the Q-junction, exerting an additive effect on flux, versus electron gating for separation of single input pathways (Hatefi et al 1962; Gnaiger 2009).**

## 6. Electron Transfer: Convergence at the Q-Junction

Proper understanding and evaluation of the functional design of the OXPHOS system requires a transition from viewing the electron transfer as a *chain* (ETC) to the recognition of the convergent structure of electron flow to the Q-junction in the electron transfer *system* (ETS; Fig. 1.5). Electron transfer capacity of cells *in vivo* is generally underestimated on the basis of the 'State 3 paradigm' and conventional respiratory protocols applied with isolated mitochondria, permeabilized cells or tissues. OXPHOS analysis extends this bioenergetic paradigm by a perspective of mitochondrial physiology emerging from a series of studies based on high-resolution respirometry (OROBOROS Oxygraph-2k).

OXPHOS analysis uses an extension of basic bioenergetic respiratory protocols, beyond the important but limited analytical potential offered by oxygen consumption measurements on intact cells. Reconstitution of citric acid cycle function in isolated mitochondria, homogenates or permeabilized cells requires the simultaneous application of CI- and CII-linked substrates. Convergent electron flow through respiratory





Complexes I and II (CI+II e-input) exerts an additive effect on respiratory flux (Fig. 1.5). OXPHOS capacities are increased up to 2-fold relative to respiratory capacity with CI- or CII-linked substrates alone. Operation of OXPHOS in top gear resolves discrepancies between intact cells and isolated mitochondria, with profound implications on evaluation of biochemical thresholds, apparent excess capacities and flux control coefficients of various mitochondrial enzyme systems. The additive effect of convergent electron input into Complexes I+II indicates a high downstream excess capacity of respiratory complexes, including cytochrome c oxidase (CIV), over the separate convergent upstream pathways through Complexes I and II (Fig. 1.5).

## 7. Biochemical thresholds and the Q-junction

The additive effect of convergent electron transfer at the Q-junction is highest when electron channelling through supercomplexes is tight (Fig. 1.5). The apparent excess capacity of a downstream step, such as the terminal cytochrome c oxidase (CIV), must then be high when related to a single input pathway (Fig. 1.6). This does not represent a functional excess capacity, however, which can only be evaluated relative to the reconstituted pathway flux (CI+II; Fig. 1.6).

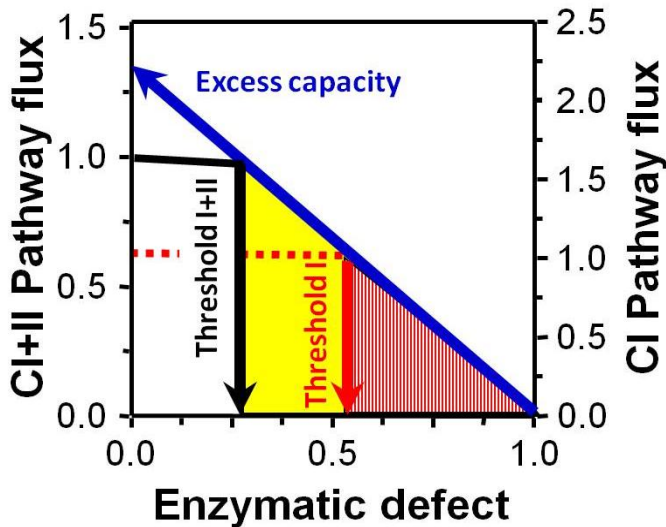


**Fig. 1.6. Biochemical threshold plot** of convergent CI+II-linked (full line, left) or CI-linked pathway flux based on electron gating (dotted line, right). A specific enzymatic defect (single step, e.g. CIV) exerts no or little effect on pathway flux (horizontal lines) up to a threshold. Beyond the threshold a linear slope is obtained, which is extrapolated to the apparent excess capacity of the single step.

Convergent CI+II e-input elicits the most pronounced stimulatory effect on coupled respiration when the phosphorylation system exerts low flux control. Convergent CI+II e-input corresponds to the operation of the citric acid cycle and mitochondrial substrate supply *in vivo*. Importantly, by establishing the reference state of maximum coupled respiration, convergent CI+II e-input provides the proper basis for (i) quantifying excess capacities of Complexes III and IV, (ii) interpreting flux control by various components such as the phosphorylation system or CIV, and (iii) for evaluation of specific enzymatic defects in the context of mitochondrial respiratory physiology and pathology.



## 8. Boundary Conditions

### 8.1. Substrate concentrations

Substrates feeding into the TCA cycle are generally added at saturating concentrations for measurement of mitochondrial respiratory capacity (Tab. A2.1), providing a buffer against substrate depletion in the course of the experiment. During exercise there is an increase in the concentrations of TCA cycle intermediates, which are not limiting in contracting skeletal muscle. An important anaplerotic reaction, replenishing the pools of metabolic intermediates in the TCA cycle, is catalyzed by pyruvate carboxylase in the mitochondrial matrix, which synthesizes oxaloacetate from pyruvate. Balanced anaplerosis and cataplerosis (entry and exit of TCA cycle intermediates) is responsible, particularly in metabolism of amino acids and gluconeogenesis (export of malate) and lipogenesis (export of citrate), for maintaining TCA cycle intermediates at steady states which shift under changing metabolic conditions of activity and starvation.

### 8.2. Respiration medium

The respiration medium MiR06 contains 10 mM inorganic phosphate ( $P_i$ ), 3 mM  $Mg^{2+}$ . Saturating ADP concentrations are added to evaluate OXPHOS capacity.  $P_i$  concentrations  $<10$  mM and  $[ADP] <0.4$  mM limit OXPHOS respiration in isolated heart mitochondria. In permeabilized muscle fibre bundles of high respiratory capacity, the apparent  $K_m$  for ADP increases up to 0.5 mM. This implies that  $>90\%$  saturation is reached only  $>5$  mM ADP, yet few studies use such high ADP concentrations in permeabilized tissues and cells. Even at saturating concentrations, flux control can be exerted by the capacity of the phosphorylation system (ATP synthase, adenine nucleotide translocase and phosphate carrier), which is indicated by noncoupled respiration in excess of OXPHOS capacity.

### 8.3. Oxygen concentration

Oxygen is not limiting for respiration of isolated mitochondria and small cells even at 20  $\mu M$  (20- to 50-fold above the apparent  $K_m$  for dissolved oxygen). In permeabilized muscle fibre bundles, however, diffusion restriction increases the sensitivity to oxygen supply 100-fold (human vastus lateralis, rat soleus and rat heart). It appears, therefore, that most studies carried out below air saturation (about 200  $\mu M$   $O_2$ ) imply oxygen limitation of OXPHOS flux in permeabilized fibres. It is recommended to apply increased oxygen levels in the range of 500 to  $>200$   $\mu M$  to studies of respiratory capacity in muscle fibres.

### 8.4. Cytochrome c retention

Release of cytochrome *c*, either under pathophysiological conditions of the cell or as a result of sample preparation, may limit active respiration. This specific effect can be separated from other OXPHOS defects by addition of



cytochrome *c* (10  $\mu\text{M}$ ), which thus provides an essential aspect of quality control of isolated mitochondria or permeabilized tissues and cells.

### 8.5. $\text{Ca}^{2+}$

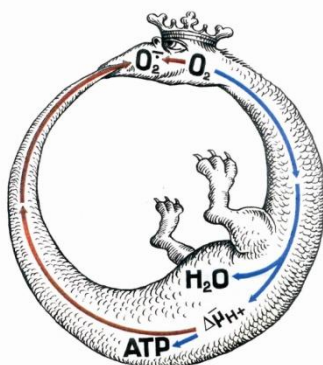
$\text{Ca}^{2+}$  at optimum concentration is an activator of dehydrogenases and oxidative phosphorylation. Free calcium in MiR05 or MiR06 is kept low by 0.5 mM EGTA. A modest increase of free calcium concentration may stimulate respiration.

### 8.6. Temperature

Experimental temperature is best chosen at or near physiological conditions, else care must be taken when extrapolating results obtained at a different temperature (Chapter 6).

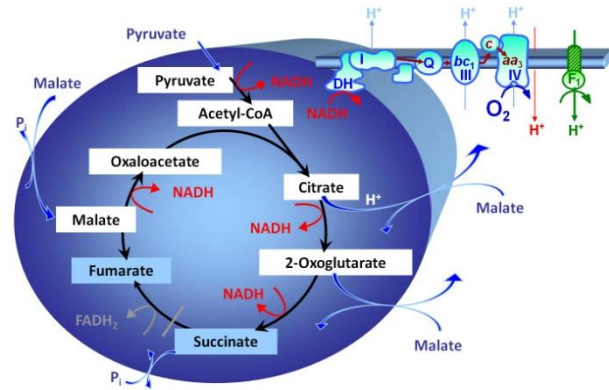
### 8.7. Sample storage

Short-term preservation of isolated mitochondria on ice in a specific preservation medium increases respiratory capacity in the ADP-activated state when compared to storage in typical isolation medium, and addition of antioxidants even in the isolation medium has a significant beneficial effect.

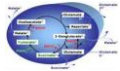




## Chapter 2. Mitochondrial Pathways to Complex I: Respiratory Substrate Control with Pyruvate, Malate and Glutamate



### Section



1. Malate .....	20
2. Pyruvate+Malate: PM .....	21
3. Glutamate .....	22
4. Glutamate+Malate: GM .....	23

Page

Mitochondrial respiration depends on a continuous flow of substrates across the mitochondrial membranes into the matrix space. Glutamate and malate are anions which cannot permeate through the lipid bilayer of membranes and hence require carriers, which is also true for pyruvate. Various anion carriers in the inner mitochondrial membrane are involved in the transport of mitochondrial metabolites. Their distribution across the mitochondrial membrane varies mainly with  $\Delta pH$  and not  $\Delta\psi$ , since most carriers (but not the glutamate-aspartate carrier) operate non-electrogenic by anion exchange or co-transport of protons.

Depending on the concentration gradients, these carriers also allow for the transport of mitochondrial metabolites from the mitochondria into the cytosol, or for the loss of intermediary metabolites into the incubation medium. Export of intermediates of the tricarboxylic acid (TCA) cycle plays an important metabolic role in the intact cell. This must be considered when interpreting the effect on respiration of specific substrates used in studies of mitochondrial preparations.

Substrate combinations of pyruvate+malate (PM) and glutamate+malate (GM) activate dehydrogenases with reduction of nicotinamide adenine dinucleotide (NADH), then feeding electrons into Complex I (NADH-UQ oxidoreductase) and down the thermodynamic cascade through the Q-cycle and Complex III of the electron transfer system to Complex IV and  $O_2$ .



## 1. Malate

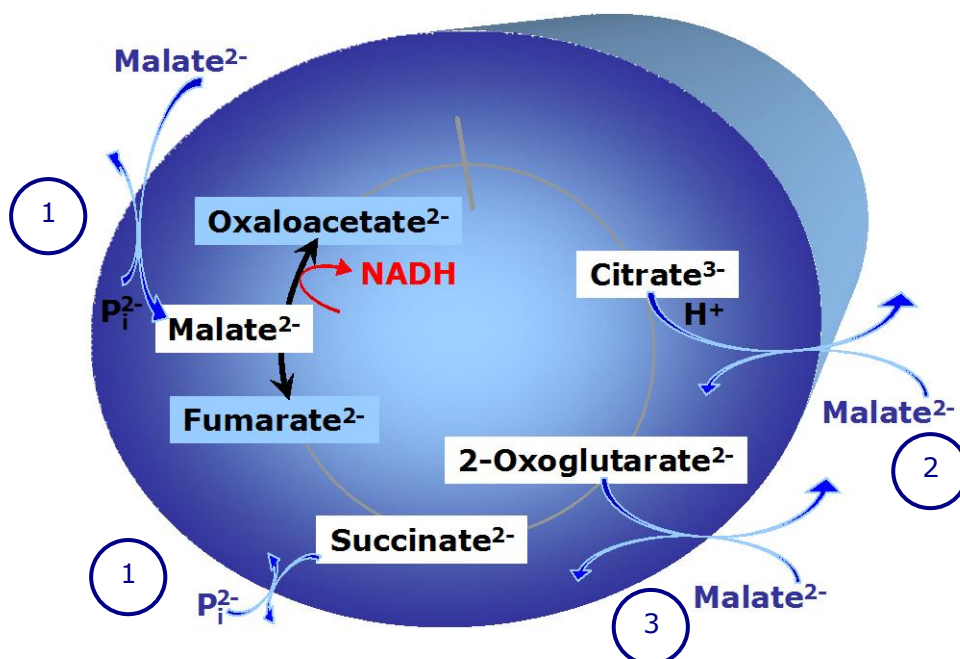


**Fig. 2.1. Malate** alone cannot support respiration of isolated mitochondria or permeabilized tissue and cells. Oxaloacetate cannot be metabolized further in the absence of a source of acetyl-CoA. Oxaloacetate cannot permeate the inner mitochondrial membrane, and accumulates. Mitochondrial citrate and 2-oxoglutarate ( $\alpha$ -ketoglutarate) are depleted by antiport with malate. Succinate is lost from the mitochondria through the dicarboxylate carrier.

### Carriers for malate

1. The dicarboxylate carrier catalyses the electroneutral exchange of malate<sup>2-</sup> or succinate<sup>2-</sup> for HPO<sub>4</sub><sup>2-</sup>. It is more active in liver than heart mitochondria.
2. The tricarboxylate carrier exchanges malate<sup>2-</sup> for citrate<sup>3-</sup> or isocitrate<sup>3-</sup> (with co-transport of H<sup>+</sup>). It is highly active in liver, but low in heart mitochondria.
3. The 2-oxoglutarate carrier exchanges malate<sup>2-</sup> for 2-oxoglutarate<sup>2-</sup>.

A significant respiratory flux with malate alone is not possible in mitochondria after depletion of endogenous substrates (Fig. 2.1). Depletion of endogenous substrates is required for evaluation of the effect of exogenously added substrates on mitochondrial respiration, and is aided by a small initial addition of ADP (State 2). Low concentrations of isolated mitochondria or small amounts of permeabilized cells or tissue may facilitate depletion of endogenous substrates. With malate alone and saturating ADP, isolated rat skeletal muscle mitochondria respire at only 1.3% of OXPHOS capacity (*P*; State 3) with pyruvate+malate.



## 2. Pyruvate+Malate: PM

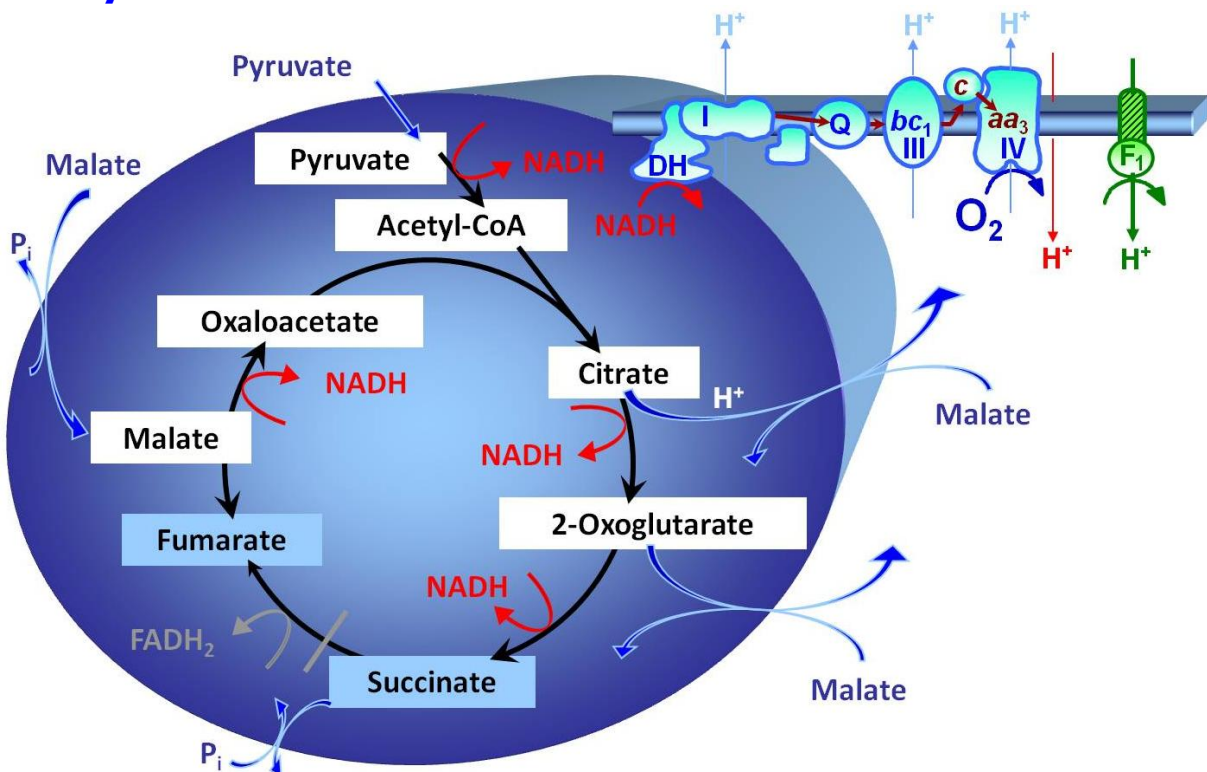


**Fig. 2.2. Pyruvate+Malate (PM).** Oxidative decarboxylation of pyruvate is catalyzed by pyruvate dehydrogenase and yields acetyl-CoA. Malate dehydrogenase located in the mitochondrial matrix oxidizes malate to oxaloacetate. Condensation of oxaloacetate with acetyl-CoA yields citrate (citrate synthase). 2-oxoglutarate ( $\alpha$ -ketoglutarate) is formed from isocitrate (isocitrate dehydrogenase).

### The pyruvate carrier

The monocarboxylic acid pyruvate<sup>-</sup> is exchanged electroneutrally for OH<sup>-</sup> by the pyruvate carrier. H<sup>+</sup>/anion symport is equivalent to OH<sup>-</sup>/anion antiport. Above a pyruvate concentration of 5 mM (compare Tab. A2.1), pyruvate transport across the membrane is partially noncarrier-mediated. Above 10 mM pyruvate, hydroxycinnamate cannot inhibit respiration from pyruvate.

Complex II is not involved in respiration on pyruvate+malate (PM) in isolated mitochondria (Fig. 2.2). The malate-fumarate equilibrium is catalyzed by fumarase with an equilibrium ratio of malate to fumarate at 4.1 in mitochondrial incubation medium. High added malate concentrations, therefore, equilibrate with fumarate, which inhibits flux from succinate to fumarate, in addition to any inhibition of succinate dehydrogenase by oxaloacetate. This prevents formation of FADH<sub>2</sub> in conjunction with the loss of 2-oxoglutarate and succinate into the medium. Due to the high activity of the tricarboxylate carrier in liver mitochondria, citrate is lost from the mitochondria in exchange for malate, before it can be oxidized. Taken together, these are the arguments of using high malate concentrations (2 mM; Tab. A2.1), particularly in



studies of P/O ratios through Complex I. Malonate may be added to inhibit the succinate-fumarate reaction, which exerts only a minor effect on liver mitochondrial respiration. Pyruvate alone yields only 2.1% of OXPHOS capacity (State *P*) with PM in rat skeletal muscle mitochondria.

Uncoupling stimulates coupled OXPHOS respiration,  $PM_p$ , by 15% in human (vastus lateralis) and rat skeletal muscle, but not in mouse skeletal muscle.

### 3. Glutamate

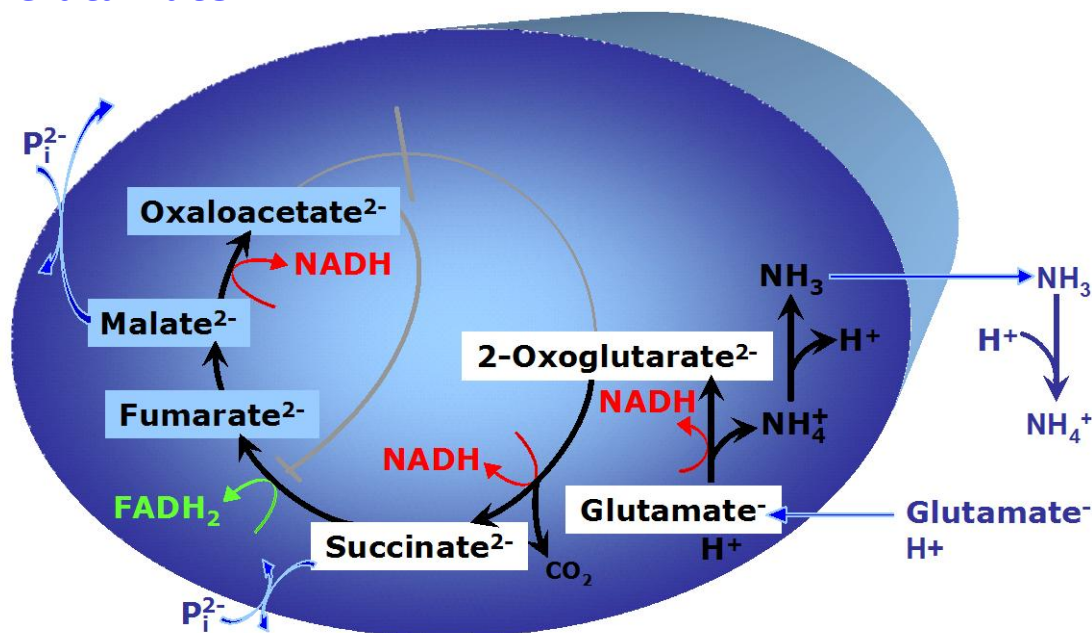


**Fig. 2.3. Glutamate** as the sole substrate is transported by the electroneutral glutamate<sup>-</sup>/OH<sup>-</sup> exchanger, and is oxidized via glutamate dehydrogenase in the mitochondrial matrix. Ammonia can pass freely through the mitochondrial membrane.

#### Carriers for glutamate

1. The glutamate-aspartate carrier catalyzes the electrogenic antiport of glutamate<sup>-</sup>+H<sup>+</sup> for aspartate<sup>-</sup>. It is an important component of the malate-aspartate shuttle in many mitochondria. Due to the symport of glutamate<sup>-</sup>+H<sup>+</sup>, the glutamate-aspartate antiport is not electroneutral and may be impaired by uncoupling. Aminooxyacetate is an inhibitor of the glutamate-aspartate carrier.
2. The electroneutral glutamate<sup>-</sup>/OH<sup>-</sup> exchanger is present in liver and kidney mitochondria.

In human skeletal muscle mitochondria, OXPHOS capacity with glutamate alone (Fig. 2.3) is 50% to 85% of respiration with glutamate+malate (Fig. 2.4). Accumulation of fumarate inhibits succinate dehydrogenase and glutamate dehydrogenase.



Glutamate derived from hydrolyzation of glutamine is a very important aerobic substrate in cultured cells. Mitochondrial glutamate dehydrogenase is particularly active in astrocytes, preventing glutamate induced neurotoxicity.

#### 4. Glutamate+Malate: GM

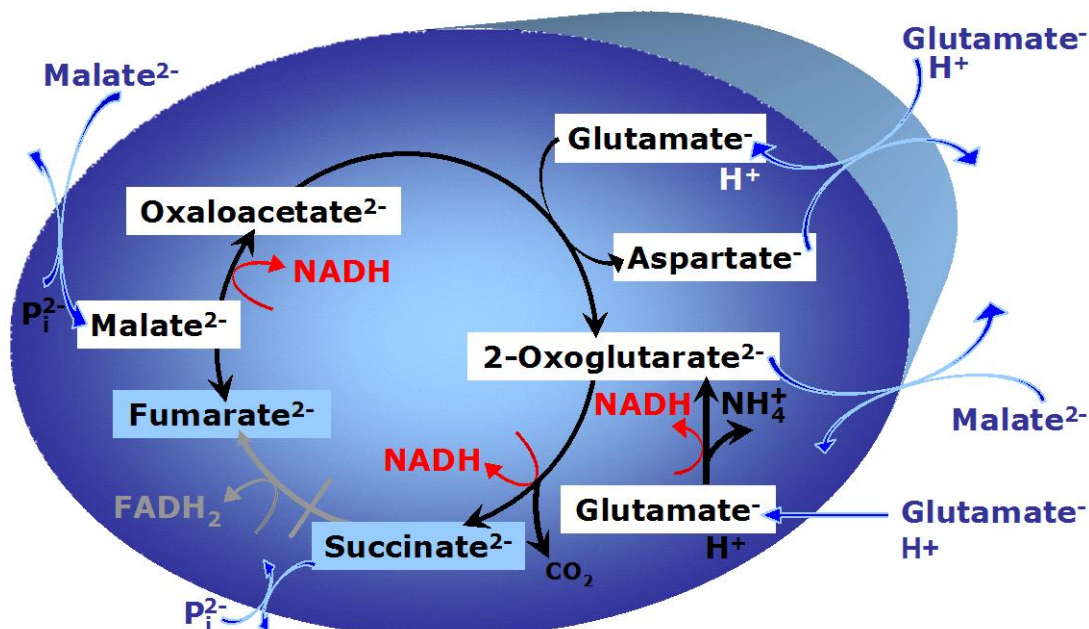


**Fig. 2.4. Glutamate+Malate (GM).** When glutamate+malate are added to isolated mitochondria or permeabilized cells, glutamate and transaminase are responsible for the metabolism of oxaloacetate, comparable to the metabolism with acetyl-CoA and citrate synthase (Fig. 2.2).

In human skeletal muscle mitochondria, respiration with glutamate+malate (Fig. 2.4) in the presence of ADP ( $GM_p$ ) is identical or 10% higher than with pyruvate+malate ( $PM_p$ ). These results on isolated mitochondria agree with permeabilized fibres, although there are reports on respiratory capacity for  $PM_p$  being 16% to 25% higher than for  $GM_p$ . In fibroblasts,  $GM_p$  supports a higher respiratory flux than  $PM_p$ .

The  $PM_p/GM_p$  flux ratio shifts from  $<1$  in white muscle to  $>1$  in red skeletal muscle fibres from turkey. In rat heart mitochondria, respiration is 33% higher for  $GM_p$  compared to  $PM_p$ , and OXPHOS with succinate+rotenone is marginally higher than with GM. 2-Oxoglutarate efflux with GM is limited at low malate concentrations, and is half-maximal at 0.36 mM. Glutamate+Malate support a higher OXPHOS respiration ( $GM_p$ ) than  $PM_p$  in rat liver mitochondria. This suggests that a critical evaluation is required for interpreting Complex I supported respiration on a particular substrate in terms of limitation by Complex I. The  $PM_p/GM_p$  ratio is strongly temperature dependent in permeabilized mouse heart fibres.





Uncoupling stimulates respiration above OXPHOS in human skeletal and cardiac muscle mitochondria, whereas respiration is not under the control of the phosphorylation system in mouse skeletal and cardiac muscle and red fibre type pigeon breast muscle mitochondria. Severe limitation was shown of  $GM_P$  (OXPHOS) respiration by the phosphorylation system in fibroblasts, since uncoupling exerts a strong stimulation above maximally ADP-stimulated respiration (compare Fig. 4.3).

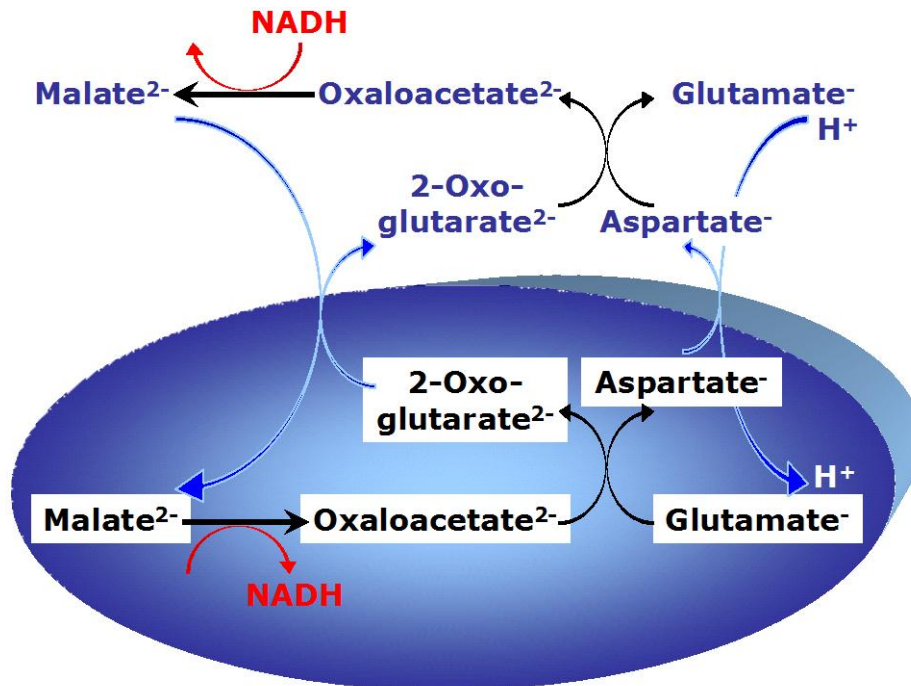
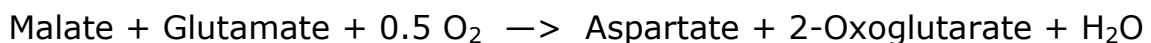
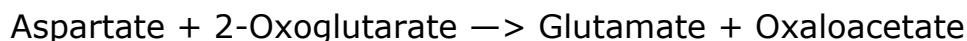


**Fig. 2.5. The malate-aspartate shuttle** involves the glutamate-aspartate carrier and the 2-oxoglutarate carrier exchanging malate<sup>2-</sup> for 2-oxoglutarate<sup>2-</sup>. Cytosolic and mitochondrial malate dehydrogenase and transaminase complete the shuttle for the transport of cytosolic NADH into the mitochondrial matrix. It is most important in heart, liver and kidney.

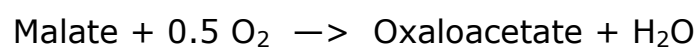
The overall reaction stoichiometry of the malate-aspartate shuttle is (Fig. 2.5):



After transamination in the cytosol (Fig. 2.6),



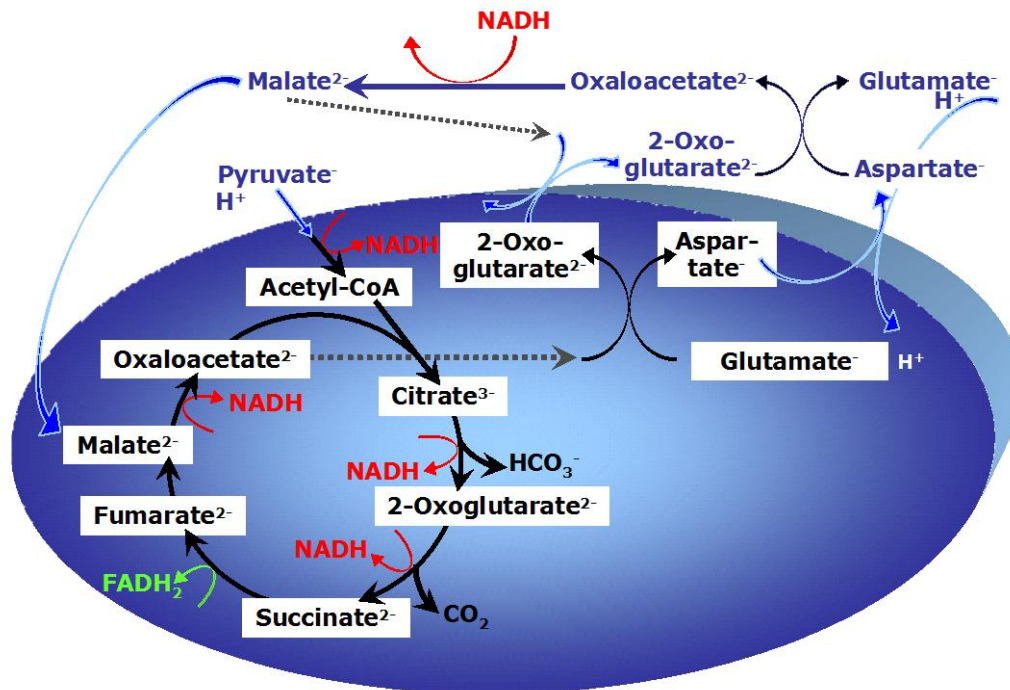
The net reaction is,



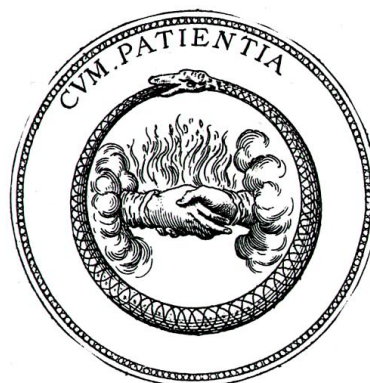
At high cardiac workload, the 2-oxoglutarate-malate transporter cannot effectively compete for the same substrate of the 2-oxoglutarate dehydrogenase, thus limiting the activity of the malate-aspartate shuttle and transfer of cytosolic NADH into the mitochondria, reducing the



cytosolic glutamate pool, and activating cytosolic reoxidation of NADH through lactate production despite sufficient oxygen availability. Regulation of cytosolic NADH levels by the glutamate-aspartate carrier is implicated in glucose-stimulated insulin secretion in beta-cells.

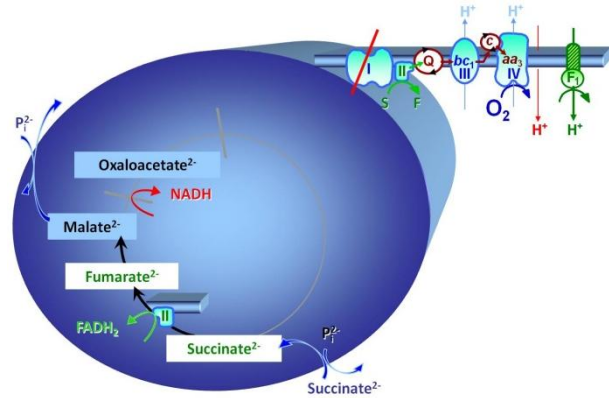


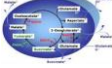
**Fig. 2.6. Malate-aspartate shuttle in the intact cell.** Cytosolic NADH is utilized for respiration at the cost of a proton transported along the electrochemical gradient back into the mitochondrial matrix. This reduces the effective P/O ratio.





## Chapter 3. Mitochondrial Pathways to Complex II, Glycerophosphate Dehydrogenase and Electron-Transferring Flavoprotein



Section		Page
	1. Succinate+Rotenone: S(Rot) .....	26
	2. Succinate: S .....	27
	3. Glycerophosphate: Gp.....	28
	4. Electron-Transferring Flavoprotein .....	28

Complex II (CII) is the only membrane-bound enzyme in the tricarboxylic acid cycle and is part of the mitochondrial electron transfer system. The flavoprotein succinate dehydrogenase is the largest polypeptide of CII, located on the matrix face of the inner mitochondrial membrane. Following succinate oxidation, the enzyme transfers electrons directly to the quinone pool. Whereas CI is NADH-linked to the dehydrogenases of the tricarboxylic acid cycle *upstream* of coenzyme Q, CII is FADH<sub>2</sub>-linked *downstream* with subsequent electron flow to Q.

### 1. Succinate+Rotenone: S(Rot)

Succinate, S(Rot), supports electron flux through CII via flavin adenine dinucleotide (FADH<sub>2</sub>). After inhibition of CI by rotenone, the NADH-linked dehydrogenases become inhibited by the redox shift from NAD<sup>+</sup> to NADH (Fig. 3.1). Succinate dehydrogenase is activated by succinate, which explains in part the time-dependent increase of respiration in isolated mitochondria after addition of succinate+rotenone and ADP.

#### Carrier for succinate

The dicarboxylate carrier catalyses the electroneutral exchange of succinate<sup>2-</sup> for HPO<sub>4</sub><sup>2-</sup>, and accumulation of malate is also prevented by exchange of malate and inorganic phosphate.

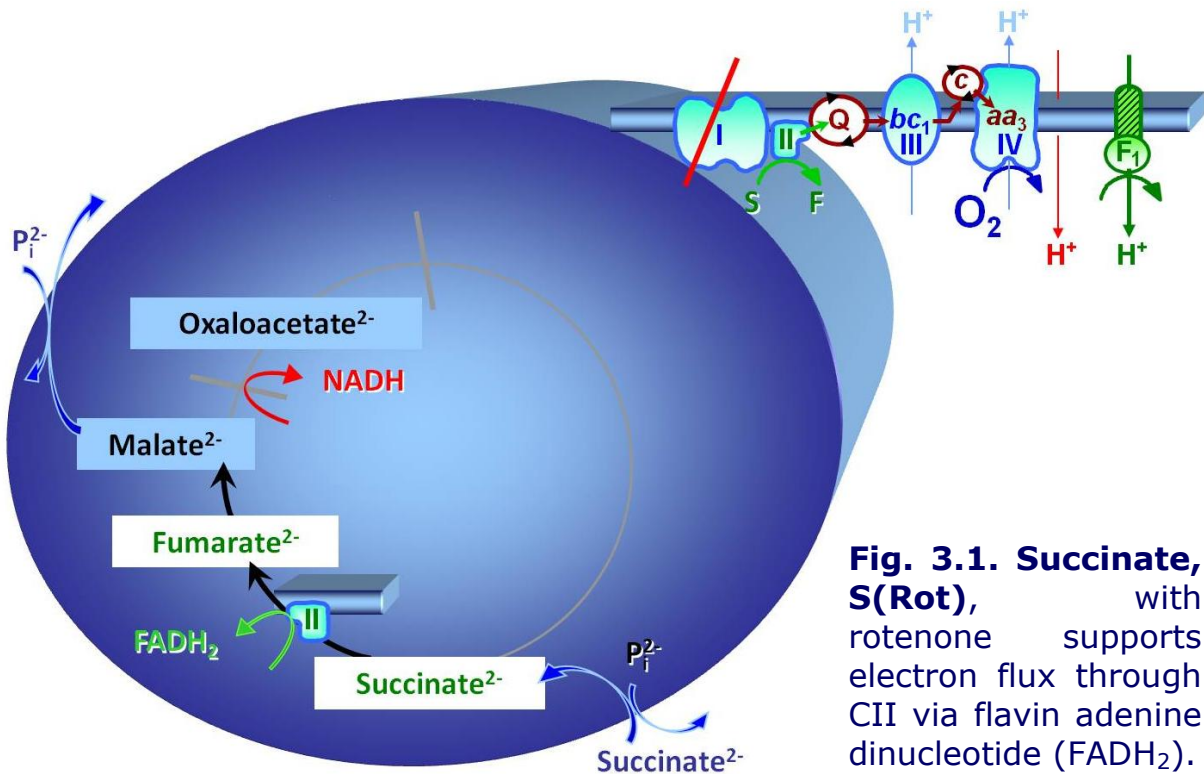


**Fig. 3.1. Succinate, S(Rot),** with rotenone supports electron flux through CII via flavin adenine dinucleotide (FADH<sub>2</sub>).

## 2. Succinate: S

When succinate is added without rotenone (Fig. 3.2), oxaloacetate is formed from malate by the action of malate dehydrogenase. Oxaloacetate cannot permeate the mitochondrial inner membrane, accumulates, and is a more potent competitive inhibitor of succinate dehydrogenase than

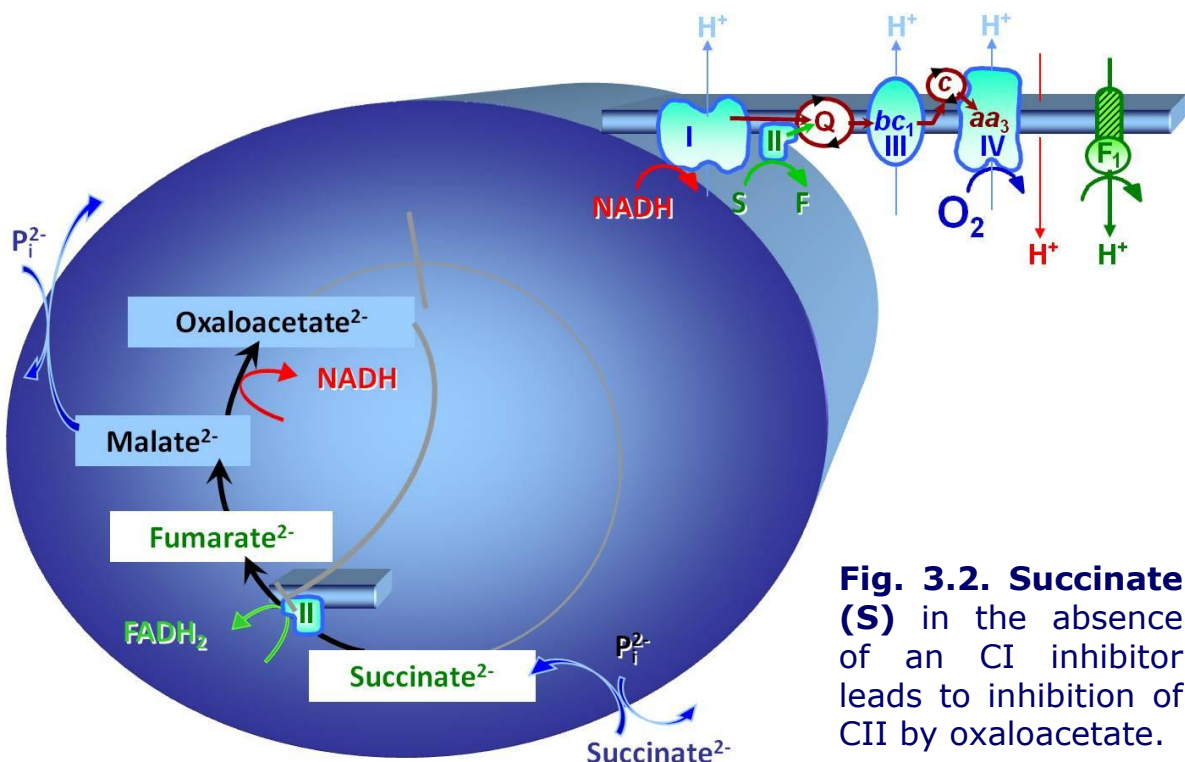


**Fig. 3.2. Succinate (S)** in the absence of an CI inhibitor leads to inhibition of CII by oxaloacetate.



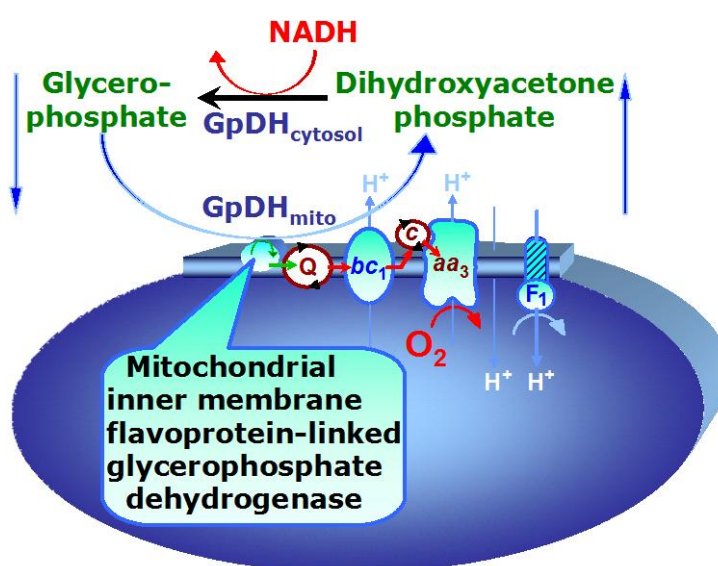
malonate even at small concentration. Reverse electron flow from CII to CI is known to stimulate production of reactive oxygen species under these conditions. Surprisingly, addition of malate inhibits superoxide production with succinate, probably due to the oxaloacetate inhibition of CII.

OXPHOS capacity with succinate alone,  $S_D$ , is underestimated at 30-40% of flux with succinate+rotenone,  $S(\text{Rot})_D$ , in human and rat skeletal muscle mitochondria, due to inhibition of succinate dehydrogenase by accumulating oxaloacetate.

### 3. Glycerophosphate: Gp

#### Fig. 3.3. The glycerophosphate shuttle

represents an important pathway, particularly in liver, of making cytoplasmic NADH available for mitochondrial oxidative phosphorylation. Cytoplasmic NADH reacts with dihydroxyacetone phosphate catalyzed by cytoplasmic glycerophosphate dehydrogenase. On the outer face of the inner mitochondrial membrane, mitochondrial glycerophosphate dehydrogenase oxidizes glycerophosphate back to dihydroxyacetone phosphate, a reaction not generating NADH but reducing a flavin prosthetic group. The reduced flavoprotein donates its reducing equivalents to the electron transfer system at the level of CoQ.



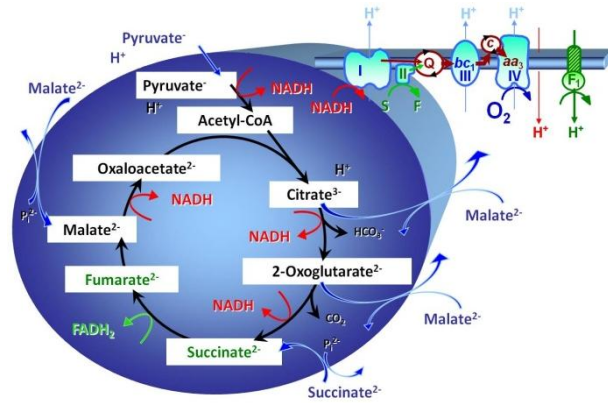
Glycerophosphate oxidation (Fig. 3.3) is 10-fold higher in rabbit gracilis mitochondria (fast-twitch white muscle; 99% type IIb) compared to soleus (slow-twitch red muscle; 98% type I). Activity is comparatively low in human vastus lateralis. Glycerophosphate is an important substrate for respiration in brown adipose tissue mitochondria.

### 4. Electron-Transferring Flavoprotein

Electron-transferring flavoprotein (ETF) is located on the matrix face of the inner mitochondrial membrane, and supplies electrons from fatty acid  $\beta$ -oxidation to CoQ.

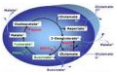


# Chapter 4. Mitochondrial Pathways to Complexes I+II: Convergent Electron Transfer at the Q- Junction and Additive Effect of Substrate Combinations



*'It is not at all easy to draw a sharp line between cases where what is happening could be called "addition", and where some other word is wanted.'*

Douglas R. Hofstadter (1979) Gödel, Escher, Bach: An Eternal Golden Braid. A metaphorical fugue on minds and machines in the spirit of Lewis Carroll. Penguin Books.

	<ol style="list-style-type: none"> <li>1. Electron Transfer System and ET Chain .....29</li> <li>2. Historical Perspectives .....32</li> <li>3. Pyruvate+Glutamate+Malate: PMG .....39</li> <li>4. Pyruvate+Malate+Succinate: PMS .....39</li> <li>5. Glutamate+Malate+Succinate: GMS.....40</li> <li>6. Pyruvate+Malate+Glutamate+Succinate: PMGS ....42</li> <li>7. Additive Effect of Gp and ETF .....42</li> <li>8. Implications .....43</li> </ol>	<p>Page</p>
--	---	-------------

## 1. Electron Transfer System and ET Chain

The term 'electron transfer chain' (or electron transport chain, ETC) is a misnomer. Understanding mitochondrial respiratory control has suffered greatly from this inappropriate terminology, although textbooks using the term ETC make it sufficiently clear that electron transfer systems are not arranged as a chain: the 'ETC' is in fact not a simple chain but an arrangement of electron transfer complexes in a non-linear, convergent electron transfer system (ETS; Fig. 4.1).

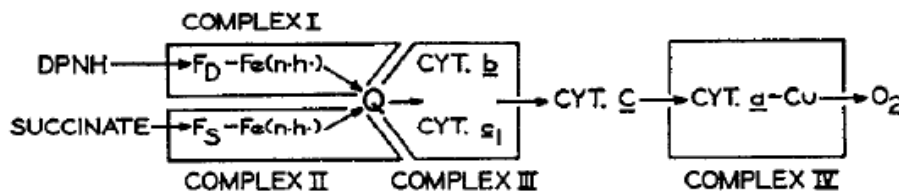


**Fig. 4.1. Electron transfer system:** The four functional primary complexes and their arrangement in the electron transfer system (Hatefi et al 1962). DPNH is NADH.

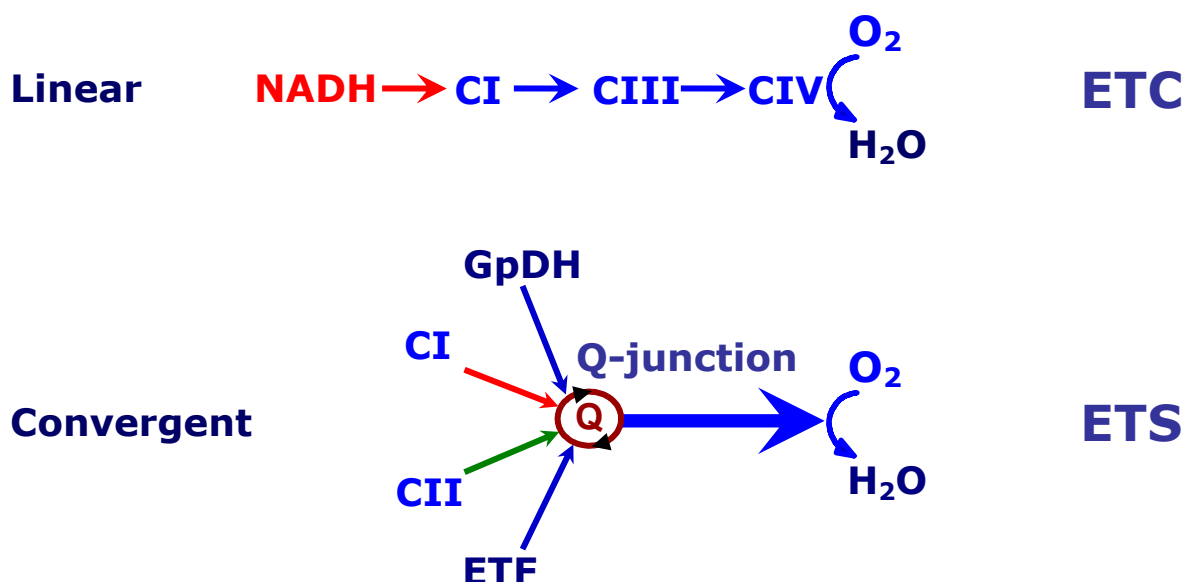


**Fig. 4.2. ETC vs ETS.** Electron transfer chain (ETC, linear) versus electron transfer system (ETS, convergent). CI to CIV, Complex I to IV; GpDH, glycerophosphate dehydrogenase; ETF, electron-transferring flavoprotein. Electron gating (ETC) limits flux upstream if convergent electron supply exerts an additive effect on ETS capacity.

The convention of defining the electron transfer chain as being comprised of four respiratory complexes has conceptual weaknesses. (a) In fact, there are at least six Complexes of mitochondrial electron transfer: In addition to Complexes I and II, glycerophosphate dehydrogenase (GpDH) and electron-transferring flavoprotein (ETF) are involved in electron transfer to Q and Complex III (Fig. 4.2). (b) The term 'chain' suggests a linear sequence, whereas the functional structure of the electron transfer system can only be understood by recognizing the convergence of electron flow at the Q-junction, followed by a chain of Complexes III and IV, mediated by cytochrome c (Fig. 4.1 and 4.2).

Electrons flow to oxygen from either Complex I (CI) with a total of three coupling sites, or from Complex II (CII) and other flavoproteins, providing multiple entries into the Q-cycle with two coupling sites downstream. A novel perspective of mitochondrial physiology and respiratory control by simultaneous supply of various substrates emerged from a series of studies based on high-resolution respirometry. Substrate-uncoupler-inhibitor-titration (SUIT) protocols for OXPHOS analysis (Fig. 4.3) are based on a biochemical analysis of convergent pathways comprising the mitochondrial electron transfer system (Fig. 4.4). When the TCA cycle is in full operation in the intact cell with influx of pyruvate, electron flow into the Q-junction converges according to a NADH:succinate ratio of 4:1 (Fig. 4.4). SUIT protocols are designed for reconstitution of TCA cycle function and sequential separation of branches of mitochondrial pathways for OXPHOS analysis.

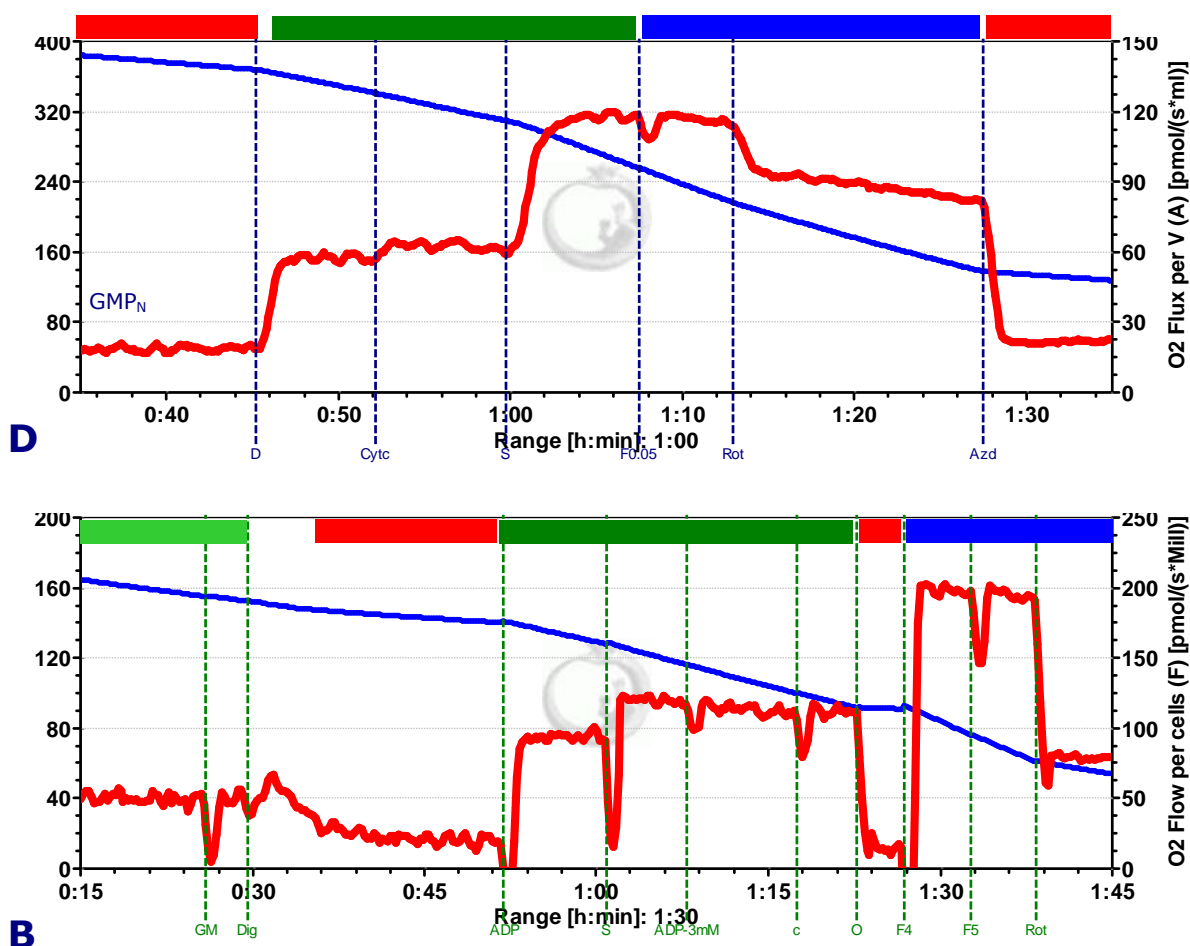


**Fig. 4.3. SUIT protocols for OXPHOS analysis.** Multiple substrate-inhibitor protocols for high-resolution respirometry in permeabilized muscle fibres and permeabilized cells. Measurements at 37 °C in the 2 ml chamber of the OROBOROS Oxygraph-2k in mitochondrial respiration medium (MiRO5). **Blue lines:** O<sub>2</sub> concentration [ $\mu$ M]; **red lines:** O<sub>2</sub> flux or flow. **A:** Permeabilized mouse skeletal muscle fibres: PGM<sub>N</sub>+D+c+S+F+Rot+Azd. PGM pyruvate+glutamate+malate, c cytochrome c, S succinate, F FCCP, Rot rotenone, Azd azide. Succinate stimulates flux two-fold, and the phosphorylation system is not limiting (no stimulation by uncoupling with F) (IOC39). **B:** Fibroblasts (NIH3T3;  $0.24 \cdot 10^6$  cells/ml): C<sub>e</sub>+GM+Dig:GM<sub>N</sub>+D+S+c+Omy+F+Rot+Ama. After measurement of routine endogenous respiration, glutamate+malate (GM) were added, and cells were permeabilized by digitonin (Dig), inducing state GM<sub>N</sub> (LEAK; no adenylates added). ADP (1 mM) stimulated respiration inducing state GM<sub>P</sub> (OXPHOS). Succinate (S) increased respiration with convergent Complex I+II electron input (GMS<sub>P</sub>). 3 mM ADP and 10  $\mu$ M cytochrome c were without stimulatory effect (GMS<sub>C<sub>P</sub></sub>). After inhibition by oligomycin (LEAK state GMS<sub>L</sub>), stimulation by FCCP (ETS state GMS<sub>E</sub>) indicated strong limitation by the phosphorylation system. Inhibition by rotenone (Rot) revealed a low capacity of respiration on succinate alone, ETS state S(Rot)<sub>E</sub>. Stimulation of coupled flux by succinate is low since the phosphorylation system exerts significant control over pathway flux indicating a high apparent ETS excess capacity.



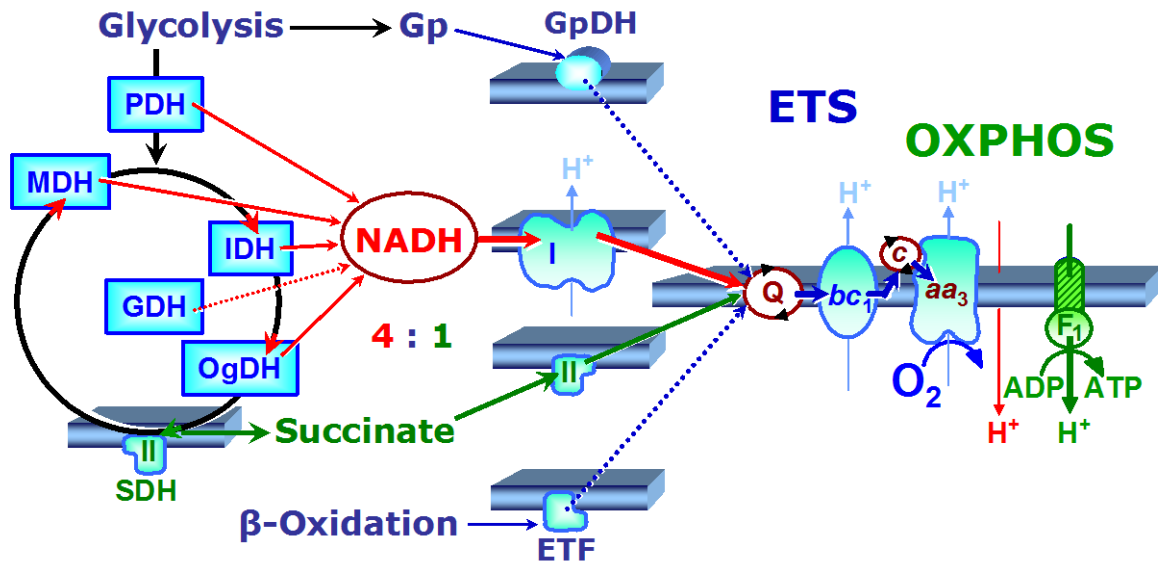


**Fig. 4.4. Convergent electron transfer** at the levels of the Q-junction (Complexes I+II, GpDH and ETF) and at the level of the NADH pool. Dehydrogenases are PDH, pyruvate DH; MDH, malate DH; IDH, isocitrate DH; OgDH, oxoglutarate DH, SDH, succinate DH - yielding a NADH:succinate ratio of 4:1 in the full TCA cycle. GDH, glutamate DH.

## 2. Historical Perspectives of Protocols with Substrate Combinations: Beyond the State 3 or ETC Paradigm of Bioenergetics

An additive effect of CI+II-linked substrate combinations was noted 50 years ago by Hatefi et al (1962). This introduced the concept of the Q-junction (Gutman et al 1971).

Convergent electron transfer through Complexes I+II is a complexity to be avoided for analyzing site-specific  $H^+$ :e and ADP:O ratios. For this aim, segments of the electron transfer system are separated into linear thermodynamic cascades, forming distinct electron transfer *chains*, using either NADH-linked substrates or the classical succinate+rotenone combination. This analytical approach pioneered by Chance and Williams (1955) is now applied mainly in the functional diagnosis of OXPHOS. The experimental separation of convergent electron transfer by electron gating is common to the extent of establishing an 'ETC paradigm of bioenergetics' in mitochondrial studies.

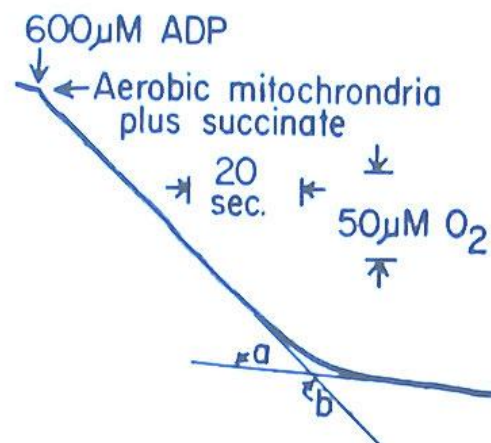


**Fig. 4.5.** Recording of the kinetics of initiation and cessation of rapid respiration in rat liver mitochondria. Chance and Williams (1955 I) Fig. 5A.



## 2.1. Intersubstrate competitions

Restriction of permeability of the inner mitochondrial membrane for various substrates of the TCA cycle raised the question on inter-substrate competition for transport, intramitochondrial concentrations and oxidation.

*Biochem. J.* (1963) **86**, 432

### Substrate Competition in the Respiration of Animal Tissues

THE METABOLIC INTERACTIONS OF PYRUVATE AND  $\alpha$ -OXOGLUTARATE  
IN RAT-LIVER HOMOGENATES

BY R. J. HASLAM\* AND H. A. KREBS

*Medical Research Council Unit for Research in Cell Metabolism, Department of Biochemistry,  
University of Oxford*

(Received 23 July 1962)

A readily oxidizable substrate—an intermediate or a starting material—often inhibits the oxidation of other substrates when added to respiring material (Krebs, 1935; Edson, 1936). In terms of enzyme chemistry this means that oxidizable substrates

\* Present address: Sir William Dunn School of Pathology, University of Oxford.

and intermediates derived from them compete with each other for the joint pathway of electron transport to molecular oxygen or for a shared co-factor. The present investigation is concerned with the detailed study of the competitive and other interactions of pyruvate,  $\alpha$ -oxoglutarate and endogenous substrates in respiring rat-liver homogenates.

Succinate accumulation is decreased by malate, and titration of phosphate or malate in the presence of succinate+rotenone progressively inhibit respiration of rat liver mitochondria (Harris and Manger 1968). In general, 'when two substrates are presented together the respiratory rate obtainable with maximal stimulation by uncoupler can exceed, be equal to or be less than the sum of the rates obtained with the respective substrates separately' (Harris and Manger 1969). Various mechanisms for explaining these different effects have been recognized, in particular that 'the stimulation of the oxidation of either malate or succinate by the addition of glutamate is due to the removal of oxaloacetate by transamination' (Harris and Manger 1969; Fig. 4.9). When  $\beta$ -hydroxybutyrate is added to NADH-linked substrates (either citrate, malate, glutamate, oxoglutarate or pyruvate), then 'with these pairs the total rate of oxidation obtainable is equal to the sum of the respective rates measured separately'. Since the 'respiratory rate obtainable from other pairs of substrates can be less than the sum of the separate rates, even though there is no known inhibition of the enzymes by the conjugate substances', the available conclusion was that 'in this circumstance mutual competition between the two anions for permeation and accumulation is presumed' (Harris and Manger 1969).

It is important to note that these investigations were based on noncoupled flux, removing any downstream limitation of flux by the phosphorylation system. Without the concepts of (i) a shift of flux control under different metabolic conditions of substrate supply to different enzyme-catalyzed steps, and (ii) convergent versus linear pathways, however, interpretation of these results on rat liver mitochondria was only



possible in terms of intersubstrate competition of substrate transport. The focus, therefore, was on inhibitory mechanisms. Although stimulation of respiration of rat liver mitochondria was observed when succinate was added to pyruvate (without succinate+rotenone as a control for an additive effect), the interpretation was that '*succinate oxidation did not inhibit pyruvate oxidation*' (König et al 1969). Although these early studies clearly showed that succinate plays an important regulatory role for mitochondrial respiration in the presence of CI-linked substrates, they appear to have had little or no influence on later concepts on mitochondrial respiratory capacity and respiratory control.

## 2.2. Scattered observations with substrate combinations

It is difficult to trace the history of observations on mitochondrial respiration with specific substrate combinations that lead to convergent electron flow through Complexes I+II (Hatefi et al 1962) or through Complex I and glycerophosphate dehydrogenase. The reason for this difficulty is related to the apparent lack of an explicit conceptual framework (Torres et al 1988), rendering valuable results scattered as observations without specific interpretation.

(i) The group of Alberto Boveris reports OXPHOS capacities ( $P$ ) with glutamate+succinate ( $GS_p$ ) which is 1.9-fold higher than glutamate+malate ( $GM_p$ ) in rat heart mitochondria (Costa et al 1988). While no values were reported for succinate+rotenone in heart, liver mitochondria were studied with succinate+rotenone,  $S(Rot)_p$ , and  $GM_p$ . The same group measured OXPHOS capacity of rat muscle and liver mitochondria in states  $GS_p$  and  $GM_p$ : The  $GM_p/GS_p$  flux ratios are 0.7 to 0.8 in liver (Llesuy et al 1994). No conclusion on an additive effect of the Complex I+II substrates is possible, since succinate(+rotenone) alone supports a higher flux than glutamate+malate in liver mitochondria and permeabilized liver tissue. In fact, the  $GM_p/S(Rot)_p$  flux ratio is 0.6 (Costa et al 1988). Similarly, the  $GM_p/GS_p$  flux ratios of 0.5 and 0.8 for rat heart and skeletal muscle mitochondria cannot be interpreted without direct comparison to flux in state  $S(Rot)_p$ .

(ii) Jackman and Willis (1996) report an additive effect of multiple substrates on flux: The sum of OXPHOS activities with glycerophosphate ( $Gp_p$ ) and pyruvate+malate ( $PM_p$ ) adds up to the respiration measured in state  $PMGp_p$ . The physiological importance of this additive effect of convergent electron flow can be evaluated only with information on the additive succinate effect, since subsequent addition of Gp may then exert a lower stimulatory effect on respiration from state  $PMS_p$  to  $PMSGp_p$ .

(iii) Kuznetsov et al (1996) note that respiration of permeabilized cardiac fibres was measured in a medium containing "10 mM glutamate + 5 mM malate as mitochondrial substrates or additionally 10 mM succinate and 0.08 mM cytochrome *c*". The fundamentally different effects of succinate and cytochrome *c* are neither distinguished nor even presented. Later, Kunz et al (2000) report a  $GM_p/GMS_p$  ratio of 0.7 in permeabilized



human muscle fibres. The apparent excess capacity of cytochrome *c* oxidase is lower with reference to the higher flux in state  $GMS_p$ , compared to the lower  $GM_p$  reference flux. This finding was interpreted by Kunz et al (2000) as a salient feature of permeabilized fibres (or intact cells) in contrast to isolated mitochondria, rather than the consequence of the multiple substrate supply. A less misguided interpretation might have been chosen with reference to the data on mitochondria isolated from rat muscle (Llesuy et al 1994), and to the  $GM_p/GS_p$  ratio of 0.5 and 0.7 for isolated mitochondria from pigeon skeletal muscle and human vastus lateralis (Rasmussen and Rasmussen 1997; 2000).

### 2.3. Maximum flux: Functional assays and noncoupled cells

(iv) Hans and Ulla Rasmussen developed the concept of 'functional assays of particular enzymes' by using various substrates and substrate combinations in respiratory studies of mitochondria isolated from skeletal muscle (Rasmussen and Rasmussen 1997; 2000). A functional assay is based on the stimulation of flux to a maximum, which then is limited by a defined system or particular enzyme. Their concept on the application of multiple substrates (glutamate+succinate) has been largely ignored in the literature, perhaps on the basis of the argument that flux control is distributed over several enzymes along a pathway. Limitation by a single enzyme, which then has a flux control coefficient of 1.0, is a rare event, even under conditions of a 'functional assay'. Importantly, however, the 1.4- or even 2.0-fold higher flux in state  $GS_p$  (Rasmussen and Rasmussen 1997; 2000) compared to the conventional State 3 paradigm (states  $PM_p$ ,  $GM_p$  and  $S(Rot)_p$ ) raises the critical issue of the physiologically appropriate reference state for measuring flux control coefficients and excess capacities of a particular enzyme such as cytochrome *c* oxidase. For general consideration, Rasmussen et al (2001) state: "The tricarboxylic acid cycle cannot be established in optimal, cyclic operation with isolated mitochondria, but parts of the *in vivo* reaction scheme may be realized in experiments with substrate combinations".

(v) Attardi and colleagues dismiss isolated mitochondria as a suitable model for respiratory studies, on the basis of the fact that 'State 3' in permeabilized cells (using Complex I-linked substrates only) is low compared to endogenous respiration of intact cells, which then "raises the critical issue of how accurately the data obtained with isolated mitochondria reflect the *in vivo* situation" (Villani and Attardi, 1997). This ignores the scattered observations on multiple substrate effects. Low OXPHOS capacity may be directly related to artefacts in the isolation of mitochondria. Thus the 'ETC paradigm of State 3' is converted into a paradigm of maximum flux, obtained by studying 'intact' cells in the noncoupled state. Whereas it is highly informative to uncouple intact cells and thus measure ETS capacity as maximum respiration, cells are not intact after uncoupling. This trivial fact is dismissed under the paradigm of maximization of flux (*italics*): "KCN titration assays, carried out on *intact uncoupled cells*, have clearly shown that the COX capacity is in low excess



(16-40%) with respect to that required to support the endogenous respiration rate" (Villani et al 1998). Uncoupling eliminates flux control by the phosphorylation system, hence the reference state of the noncoupled cell is nonphysiological, unless the phosphorylation system exerts no control over coupled respiration.

## 2.4. Mitochondrial Physiology and Mitochondrial Pathways

A rapidly growing number of studies on various tissues and cells points to the importance of the additive effect of substrate combinations on OXPHOS capacity (Gnaiger 2009). Convergent CI+II electron flow to the Q-junction resolves discrepancies between intact cells and mitochondria. This additive effect indicates a high downstream excess capacity of respiratory complexes including cytochrome *c* oxidase (CIV) over Complexes I and II. Convergent electron transfer yields a maximum (additive) effect on OXPHOS when cytochrome *c* oxidase and the phosphorylation system exert a minimum (zero) flux control. Convergent electron transfer corresponds to the operation of the TCA cycle and mitochondrial substrate supply *in vivo*. In isolated mitochondria and permeabilized cells or tissue, conventional measurements of State 3 with pyruvate+malate, glutamate+malate or succinate+rotenone underestimate OXPHOS capacity, since external succinate is required for reconstitution of the TCA cycle and stimulating convergent CI+II electron flow under these conditions. By establishing the physiological reference state of maximum *coupled* respiration, convergent CI+II electron flow provides the proper basis for (i) quantifying excess capacities and interpreting flux control by various enzymes such as cytochrome *c* oxidase and components such as the phosphorylation system, and (ii) evaluation of specific enzymatic defects in mitochondrial respiratory physiology and pathology (Fig. 1.6). The concept on convergent electron transfer at the Q-junction (ETS) challenges conventional OXPHOS analysis based on the ETC terminology and a way of thinking about the mitochondrial 'electron transfer chain' (Fig. 4.2).

OXPHOS capacity (*P*; coupled) over ETS capacity (*E*; noncoupled) is the *P/E* coupling control ratio. The *P/E* ratio yields important information on the limitation of OXPHOS capacity by the phosphorylation system. Electron gating (ETC) limits flux artificially upstream of the Q-junction, thereby obscuring the quantitative importance of physiological flux control by the phosphorylation system (Fig. 4.4).

Specifically designed substrate-uncoupler-inhibitor titrations (SUIT) extend experimental protocols for OXPHOS analysis in the diagnosis of mitochondrial respiratory function. An important added value of SUIT protocols is the sequential measurement of mitochondrial function in multiple respiratory states of substrate and coupling control (Fig. 4.3; 4.6 to 4.8). This increases the information obtained from a limited amount of biological sample and allows the calculation of statistically robust internal flux control ratios, in contrast to the separate assays applied previously.

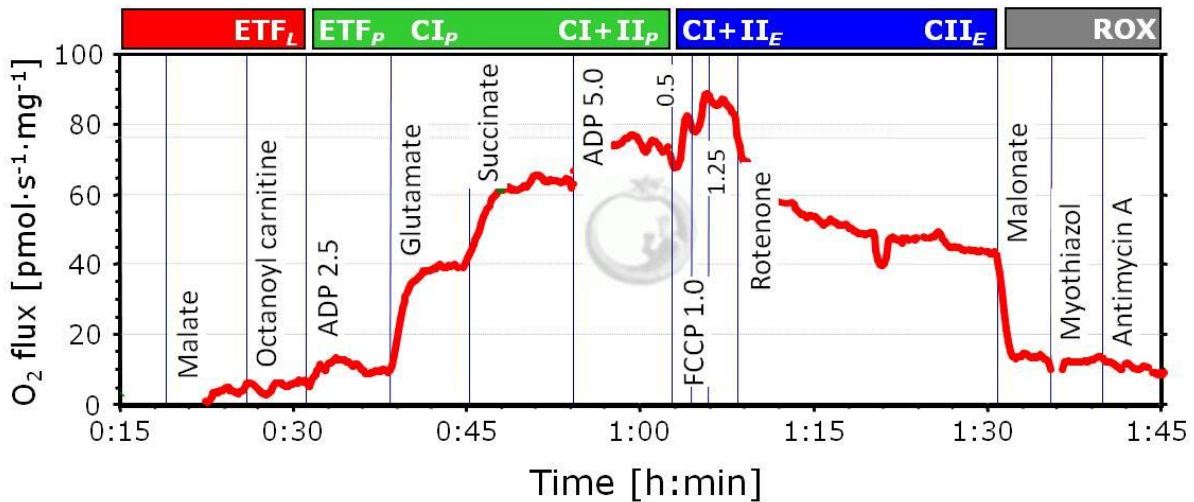


**Fig. 4.6. SUIT protocols for OXPHOS analysis: Human vastus lateralis. A:** Mass-specific oxygen flux [ $\text{pmol O}_2 \cdot \text{s}^{-1} \cdot \text{mg}^{-1} W_w$ ] with substrates for electron-transferring flavoprotein (ETF), Complex I (CI), and Complex II (CII). Permeabilized fibres, 2.8 mg  $W_w$ ; 37 °C, MiR06, 2 ml chamber; experiment 2010-03-04 CD-01 (Pesta, Gnaiger 2012).

Protocol:  $\text{OctM}_N + \text{D}_{2.5} + \text{G} + \text{S} + \text{D}_5 + \text{F}_{=1.25} + \text{Rot} + \text{Mna} + \text{Myx} + \text{Ama}$ .

1.  $\text{OctM}_N$ :  $(\text{ETF} + \text{CI})_L$  in the LEAK state  $L$  (no adenylates,  $N$ ).
2.  $\text{OctM}_{\text{D}2.5}$ :  $(\text{ETF} + \text{CI})_P$ , OXPHOS state  $P$  (2.5 mM ADP).
3.  $\text{GMOct}_{\text{D}2.5}$ :  $(\text{CI} + \text{ETF})_{\text{D}2.5}$ , OXPHOS is ADP-limited at 2.5 mM.
4.  $\text{GMSOct}_{\text{D}2.5}$ :  $(\text{CI} + \text{II} + \text{ETF})_{\text{D}2.5}$ .
5.  $\text{GMSOct}_{\text{D}5}$ :  $(\text{CI} + \text{II} + \text{ETF})_P$ , OXPHOS capacity at 5 mM ADP.
6.  $\text{GMSOct}_E$ :  $(\text{CI} + \text{II} + \text{ETF})_E$ , ETS capacity after FCCP titration to 1.25  $\mu\text{M}$ .
7.  $S(\text{Rot})_E$ :  $\text{CII}_E$ .
8.  $(\text{Mna} + \text{Myx} + \text{Ama})_{\text{ROX}}$ : residual oxygen consumption, ROX.

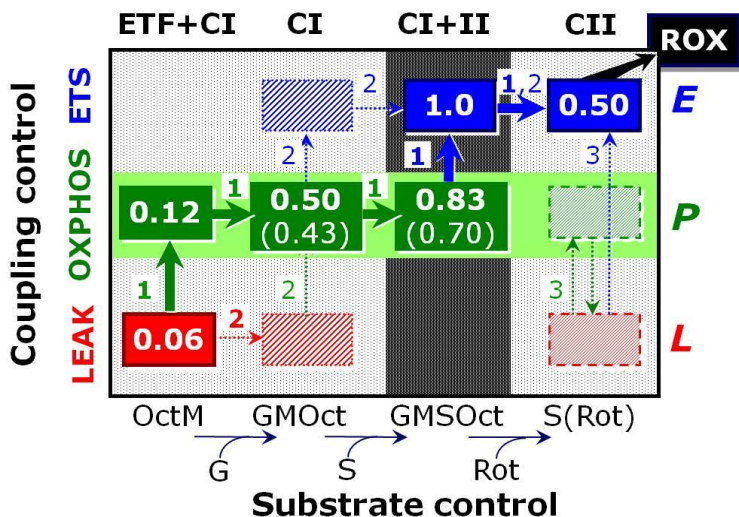


**Fig. 4.7. Coupling/substrate control diagram** with flux control ratios ( $FCR$ ) normalized relative to ETS capacity with convergent CI+II electron input (arrows 1, corresponding to panel A;  $FCR$  in parentheses are pseudo-state  $P$  at 2.5 mM ADP). Additional protocols (arrows 2 and 3) are required to fill in the dashed coupling/substrate states,

including overlapping respiratory state  $S(\text{Rot})_E$  in all cases (2:  $\text{OctM}_N + \text{G} + \text{D} + \text{F} + \text{S} + \text{Rot}$ ; 3:  $\text{Rot} + \text{S} + \text{D} + \text{F}$ ). Residual oxygen consumption (ROX) is determined as a common step in the three protocols on integrated pathways (+Mna+Myx+Ama); see Appenix for abbreviations (Pesta, Gnaiger 2012).

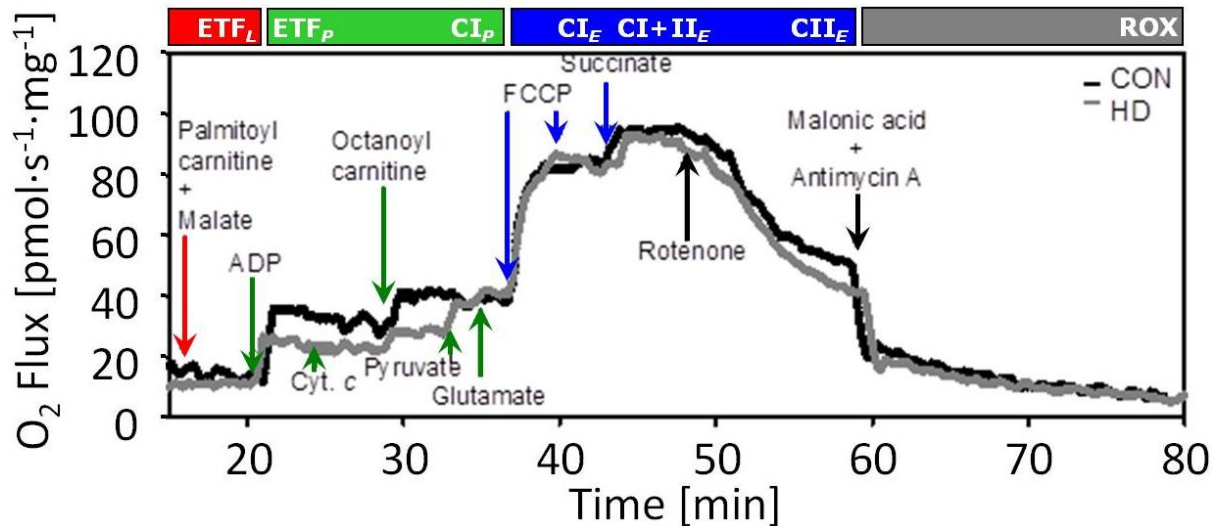


**Fig. 4.8. SUIIT protocols for OXPHOS analysis: Human heart.** permeabilized myocardial fibres from healthy controls fatty acid SUIIT protocol for electron flux through electron-transferring flavoprotein+Complex I (ETF+CI). After addition of pyruvate+glutamate, the predominant electron flux is through CI (CI+ETF). Superimposed traces are shown of tissue mass-specific respiratory flux as a function of time for a control and heart disease patient (CON and HD; 2.1 and 1.8 mg fibre wet weight per chamber). Arrows indicate titrations, identical for both traces; continued with ascorbate+TMPD (from Lemieux et al 2011).

Protocol: **PaIM<sub>N</sub>+D+c+Oct+P+G+F+S+Rot+Mna+Ama.**

1. **PaIM<sub>N</sub>**: (ETF+CI)<sub>L</sub> in the LEAK state *L* (no adenylates, *N*).
2. **PaIM<sub>P</sub>**: (ETF+CI)<sub>P</sub>, OXPHOS state *P* (2.5 mM ADP, saturating).
3. **PaIMc<sub>P</sub>**: (ETF+CI)<sub>P</sub>, state *P* with cytochrome *c*.
4. **PaIOctM<sub>P</sub>**: (ETF+CI)<sub>P</sub>.
5. **PMPaIOct<sub>P</sub>**: (CI+ETF)<sub>P</sub>.
6. **PMGPaIOct<sub>P</sub>**: (CI+ETF)<sub>P</sub>.
7. **PMGPaIOct<sub>E</sub>**: (CI+ETF)<sub>E</sub>, ETS state *E*, capacity after FCCP titration.
8. **PMGSPaIOct<sub>E</sub>**: (CI+II+ETF)<sub>E</sub>.
9. **S(Rot)<sub>E</sub>**: CII<sub>E</sub>.
10. (Mna+Myx+Ama)<sub>ROX</sub>: residual oxygen consumption, ROX.

Human skeletal and cardiac muscle are compared in Fig. 4.6 and 4.8. Note the pronounced additive effect of CI+II-linked respiration in skeletal muscle (as well as in mouse skeletal muscle and human fibroblasts, Fig. 4.3). In contrast, human heart mitochondria show a minor additive effect upon addition of succinate to the CI-substrate state, whereas the *P/E* coupling control ratio is significantly higher in skeletal muscle mitochondria (smaller uncoupling effect, Fig. 4.6) and *P/E* is 1.0 in mouse muscle (Fig. 4.3A). The OXPHOS flux control pattern of human fibroblasts (Fig. 4.3B) is more comparable to the human heart and human skeletal muscle, but very different from mouse skeletal muscle (Fig. 4.3A). For a detailed discussion of these SUIIT protocols see Lemieux et al (2011), Pesta et al (2011), Pesta and Gnaiger (2012) and Votion et al (2012).



### 3. Pyruvate+Malate+Glutamate: PMG

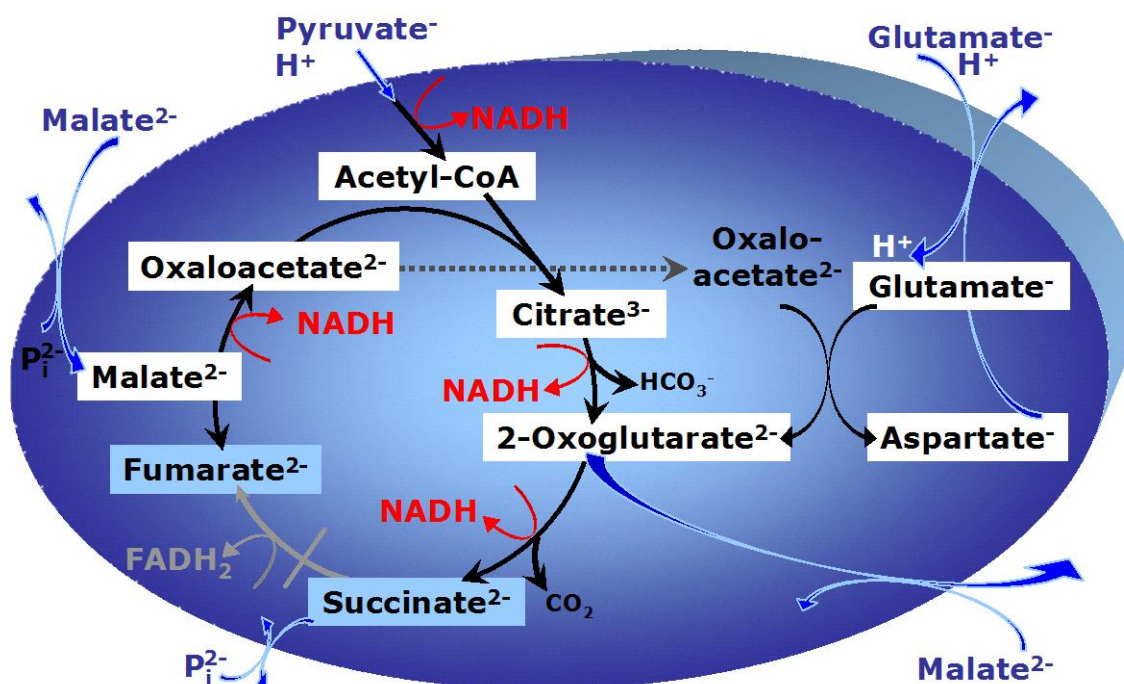


**Fig. 4.9. PMG.** Respiratory capacity through Complex I may be limited by substrate supply. The addition of pyruvate and glutamate with malate (PMG; compare Fig. 4.4) yields respiration in the presence of both pyruvate and the malate-aspartate shuttle.

Mitochondria from red muscle fibres (rabbit soleus) exhibit a 15% higher flux in state  $PMG_p$  (Fig. 4.9) compared to  $PM_p$ , whereas white muscle fibre mitochondria (rabbit gracilis) show a slight inhibition by glutamate added to  $PM_p$  (Jackman and Willis 1996). Paradoxically, a significant inhibition of flux by addition of pyruvate to  $GM_p$  was observed in horse skeletal muscle fibres (Votion et al 2012). Addition of glutamate to pyruvate+malate increases respiratory capacity in human skeletal muscle (Winkler-Stuck et al 2005; although  $PM_p$  is 16% higher than  $GM_p$ ). There is a strong additive effect of the PMG-substrate combination on respiratory capacity of mouse heart fibres (Lemieux et al 2006).

### 4. Pyruvate+Malate+Succinate: PMS

Reconstitution of TCA cycle function in isolated mitochondria or permeabilized tissues and cells requires addition of succinate to the conventional substrates for Complex I (Fig. 4.10). The TCA cycle is functionally not 'closed' when using the substrate combination pyruvate+malate, when citrate and 2-oxoglutarate are exchanged rapidly for malate by the tricarboxylate and 2-oxoglutarate carrier (Fig. 2.2). Then succinate dehydrogenase activity is fully dependent on a high external succinate concentration.



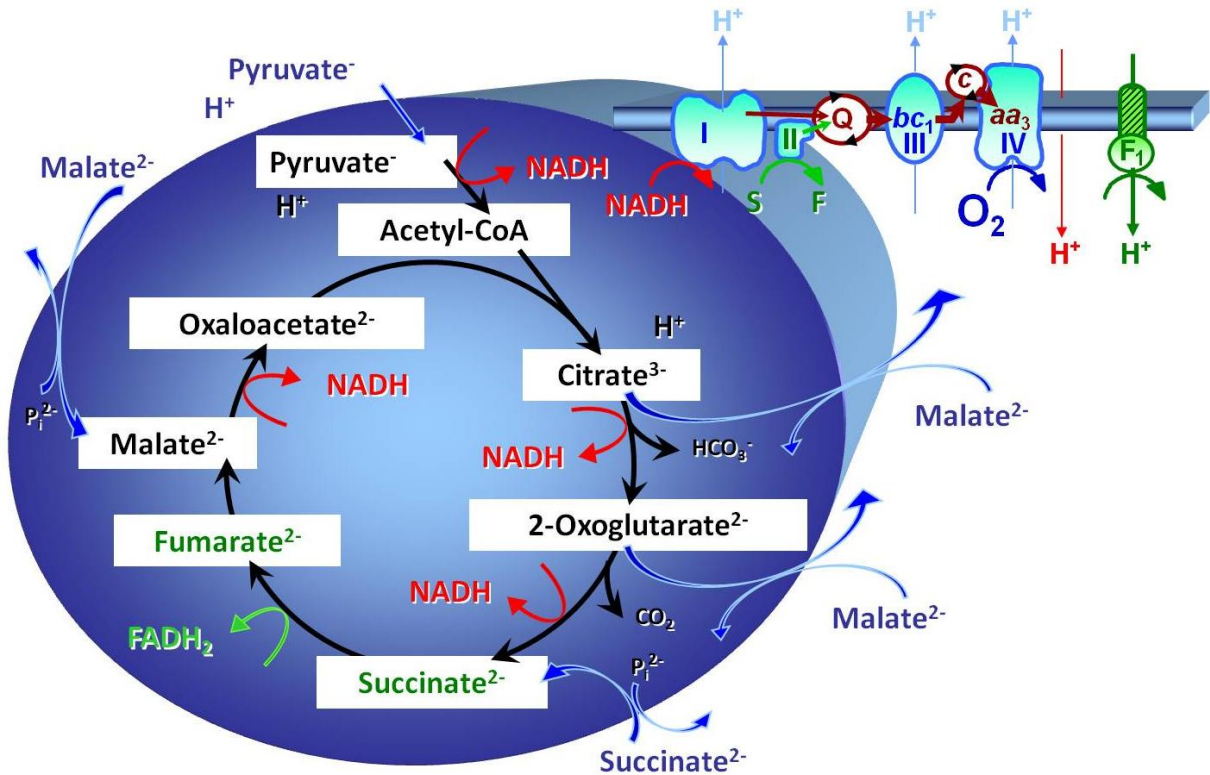


**Fig. 4.10. PMS.** Convergent electron flow to the Q-junction with substrate combination pyruvate+malate+succinate (PMS).

### 5. Glutamate+Malate+Succinate: GMS

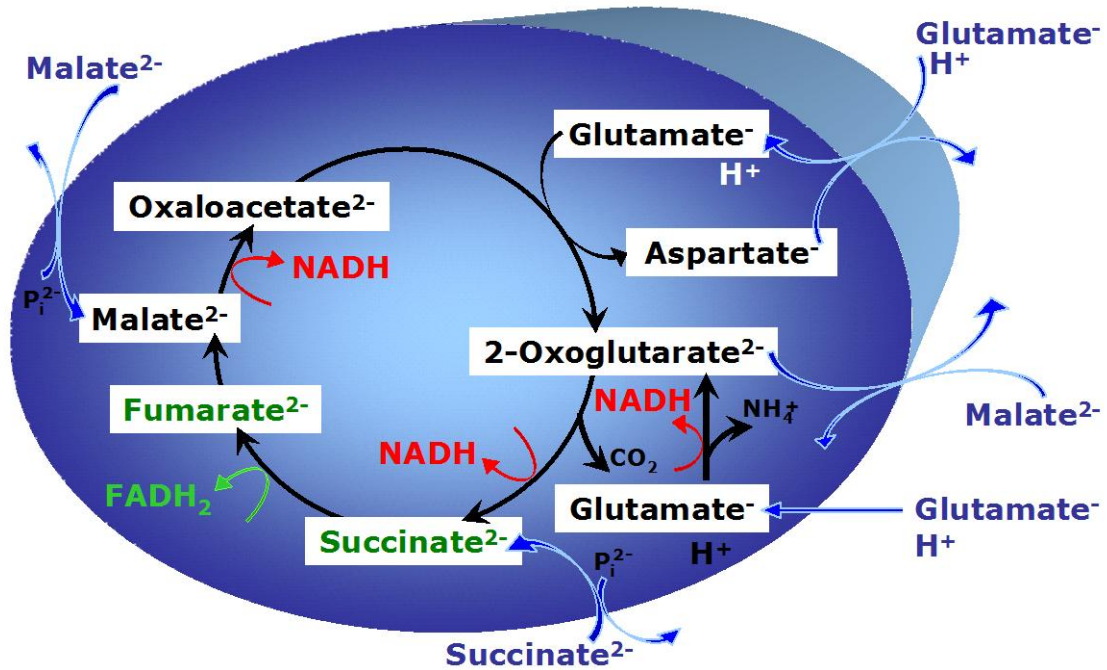


**Fig. 4.11. GMS.** Convergent electron flow to the Q-junction with substrate combination glutamate+malate+succinate (GMS).

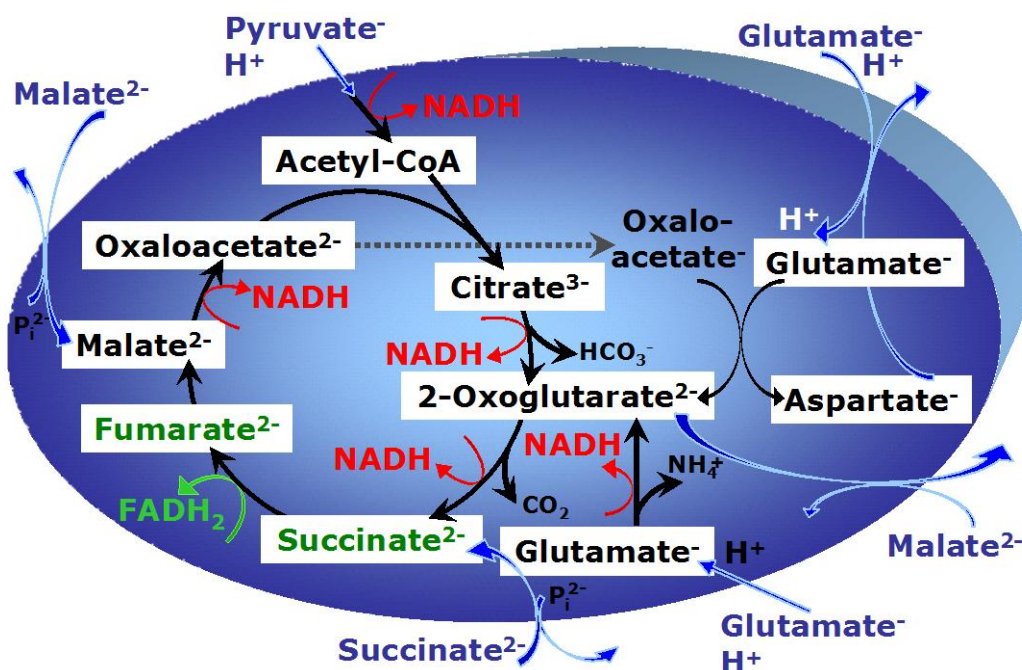


**Fig. 4.12. PMGS:** Convergent electron flow to the Q-junction with substrate combination pyruvate+malate+glutamate+succinate (PMGS).

Transaminase catalyzes the reaction from oxaloacetate to 2-oxoglutarate, which then establishes a cycle without generation of citrate. OXPHOS is higher with glutamate+succinate (CI+II) compared to glutamate+malate (CI) or succinate+rotenone (CII). This documents an additive effect of convergent electron flow from Complexes I+II to the Q-junction, with consistent results obtained with permeabilized muscle fibres and isolated mitochondria (Gnaiger 2009). In human skeletal muscle mitochondria (25 °C), Rasmussen and Rasmussen (2000) obtained CI/CI+II flux ratios of 0.7 (0.6) for OXPHOS (or ETS) with glutamate+malate (8+4 mM) and glutamate+succinate (4+8 mM), and CII/CI+II flux ratios of 0.8 (0.6) for OXPHOS (or ETS). Since glutamate alone supported only 49% of OXPHOS flux with glutamate+malate, addition of malate to their glutamate+succinate assay would have been of interest. The  $GM_P/GMS_E$  and  $S(Rot)_E/GMS_E$  flux control ratios are 0.50 and 0.55 in human vastus lateralis (Pesta et al 2011).

Due to the lower  $H^+/O_2$  stoichiometry in succinate respiration compared to CI-linked respiration (two versus three coupling sites), the CI/CI+II ratio is lower for LEAK respiration (0.3 to 0.4; Garait et al 2005) compared to OXPHOS.

In human skeletal muscle, the phosphorylation system is more limiting at the highest OXPHOS activity with glutamate+succinate, at a  $P/E$  ratio ( $GS_P/GS_E$ ) of 0.69 versus 0.80 with glutamate+malate (Rasmussen and Rasmussen 2000). Failure of obtaining a further stimulation of coupled OXPHOS in human skeletal muscle mitochondria with GMS by uncoupling (Kunz et al 2000) can be explained by the high



FCCP concentration applied (10  $\mu\text{M}$ ) which is known to inhibit respiration (Steinlechner-Maran et al 1996). In mouse skeletal muscle, however, the *P/E* ratio is actually 1.0 (Aragones et al 2008), which contrasts with the significant limitation of OXPHOS capacity by the phosphorylation system in humans (Fig. 4.3B, 4.6 and 4.8).

## 6. Pyruvate+Malate+Glutamate+Succinate: PMGS

2-oxoglutarate is produced through the citric acid cycle from citrate by isocitrate dehydrogenase, from oxaloacetate and glutamate by the transaminase, and from glutamate by the glutamate dehydrogenase. If the 2-oxoglutarate carrier does not outcompete these sources of 2-oxoglutarate, then the TCA cycle operates in full circle with external pyruvate+malate+glutamate+succinate (Fig. 4.12).

## 7. Additive Effect of Glycerophosphate Dehydrogenase and Electron-Transferring Flavoprotein

On the outer face of the inner mitochondrial membrane, mitochondrial glycerophosphate dehydrogenase oxidizes glycerophosphate to dihydroxyacetone phosphate, reducing a flavin prosthetic group that donates its reducing equivalents to the electron transfer system at the level of CoQ. Electron-transferring flavoprotein (ETF) is located on the matrix face of the inner mitochondrial membrane, and supplies electrons from fatty acid  $\beta$ -oxidation to CoQ.

Glycerophosphate oxidation is 10-fold greater in rabbit gracilis mitochondria (fast-twitch white muscle; 99% type IIb) compared to soleus (slow-twitch red muscle; 98% type I). Both types of skeletal muscle mitochondria exhibit additive pyruvate and glycerophosphate oxidase activities (Jackman and Willis 1996).

Oxygen flux in the presence of glycerophosphate is increased by subsequent addition of succinate to brown adipose tissue mitochondria (Rauchova et al 2003). It has yet to be shown if there is an additive effect of applying these two substrates, or if succinate+rotenone respiratory capacity is already sufficient for supporting the maximum flux.

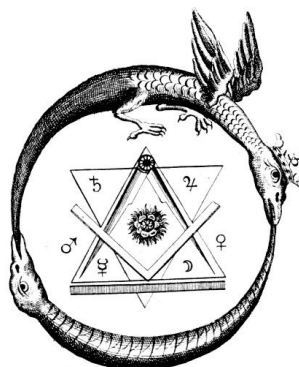
Red and white rabbit muscle mitochondrial respiration is slightly increased when palmitoylcarnitine is added to  $\text{PM}_p$  (Jackman and Willis 1996). Similarly, ATP production in mitochondria isolated from human muscle is higher with a substrate combination (malate+pyruvate+2-oxoglutarate+palmitoylcarnitine) that supports convergent electron input into the Q-junction through Complex I and ETF, than with electron input into either Complex I or II (Tonkonogi et al 1999; Short et al 2005).

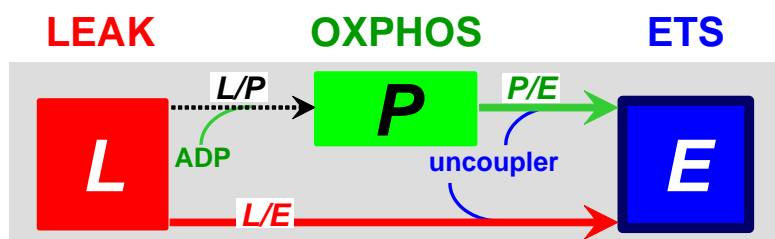


## 8. Implications

Application of physiological substrate combinations is a hallmark of the extension of mitochondrial bioenergetics to mitochondrial physiology and OXPHOS analysis. Conventional studies with various substrates for NADH-related dehydrogenases prevent the simultaneous activation of Complex II or other convergent pathways into the Q-junction (Fig. 4.4). Convergent electron input into the Q-cycle characterizes mitochondrial function *in vivo*, with a minimum of 1/5<sup>th</sup> to 1/4<sup>th</sup> of electron flow through Complex II even for respiration on pure carbohydrate.

- (i) For appreciation of the diversity of mitochondrial function in different animals and tissues, mitochondrial respiratory capacity has to be generally re-assessed with application of substrate combinations appropriate for a complete operation of the citric acid cycle.
- (ii) Interpretation of excess capacities of various components of the electron transfer system and of flux control coefficients is largely dependent on the metabolic reference state. Appreciation of the concept of the Q-junction will provide new insights into the functional design of the respiratory system.
- (iii) The conventional view of a drop of mitochondrial membrane potential with an increase of flux from the LEAK to OXPHOS state (high to moderate membrane potential) has to be modified, based on the appreciation of the important control of flux by substrate supply. The relation between membrane potential and flux is reversed when an increase in flux is affected by a change in substrate supply.
- (iv) Based on the relationship between ROS production and reversed electron flow from Complex II to Complex I, multiple substrates have been supplied in investigations of oxidative stress related to mitochondrial metabolism. The dependence of ROS production on membrane potential and metabolic state will have to be investigated further, to resolve pertinent controversies on the role of mitochondria in cellular ROS production.
- (v) Supercomplex formation, metabolic channelling and partially additive effects on flux suggest that convergent electron input into the Q-junction only partially proceeds through a common CoQ pool.





## Chapter 5. Respiratory States, Coupling Control and Coupling Control Ratios

'The growth of any discipline depends on the ability to communicate and develop ideas, and this in turn relies on a language which is sufficiently detailed and flexible.'

Simon Singh (1997) Fermat's last theorem. Fourth Estate, London.

Section		Page
	1. Coupling in Oxidative Phosphorylation .....	44
	2. Respiratory Steady-States .....	45
	2.1 Leak Respiration, <i>L</i> .....	47
	2.2 Oxphos Capacity, <i>P</i> .....	48
	2.3 Electron Transfer System Capacity, <i>E</i> .....	48
	2.4 Respiratory States of the Intact Cell .....	48
	3. Coupling Control Ratios (CCR) .....	49

### 1. Coupling in Oxidative Phosphorylation

In oxidative phosphorylation, the endergonic process of phosphorylation of ADP to ATP is coupled to the exergonic process of electron transfer to oxygen. Coupling is achieved through the proton pumps generating and utilizing the protonmotive force in a proton circuit across the inner mitochondrial membrane. This proton circuit is partially uncoupled by proton leaks (Fig. 1.1). The coupling state (or uncoupling state) of mitochondria is a key component of mitochondrial respiratory control. Three different meanings of uncoupling (or coupling) are distinguished by defining intrinsically **uncoupled**, pathologically **dyscoupled**, and experimentally **noncoupled** respiration:

1. In partially uncoupled (or partially coupled) respiration, *intrinsic uncoupling* under physiological conditions is a property of the inner mt-membrane (proton leak), proton pumps (proton slip; decoupling), and molecular uncouplers (uncoupling protein, UCP1).

2. *Dyscoupled* respiration under pathological and toxicological conditions is related to mitochondrial dysfunction. An explicit distinction is made between physiologically regulated uncoupling and pathologically defective dyscoupling (analogous to distinguishing eustress versus distress, function versus dysfunction).

3. *Noncoupled* respiration in the experimentally controlled fully uncoupled ( $\equiv$ noncoupled) state is induced by application of established uncouplers (protonophores, such as FCCP or DNP), with the aim of obtaining a reference state with reduced mt-membrane potential, for



evaluation of the respiratory capacity through the electron transfer system, or a defined state for measurement of mt-ROS production.

Experimentally available uncouplers are protonophores which do not uncouple electron transfer from proton translocation, but generate an artificially increased proton leak as a bypass of coupled ATP synthesis (Fig. 1.1).

## 2. Respiratory Steady-States

Respiratory steady states have been defined by Chance and Williams (1955 I, III) according to a protocol for oxygraphic experiments with isolated mitochondria (Fig. 5.1; Tab 5.1).

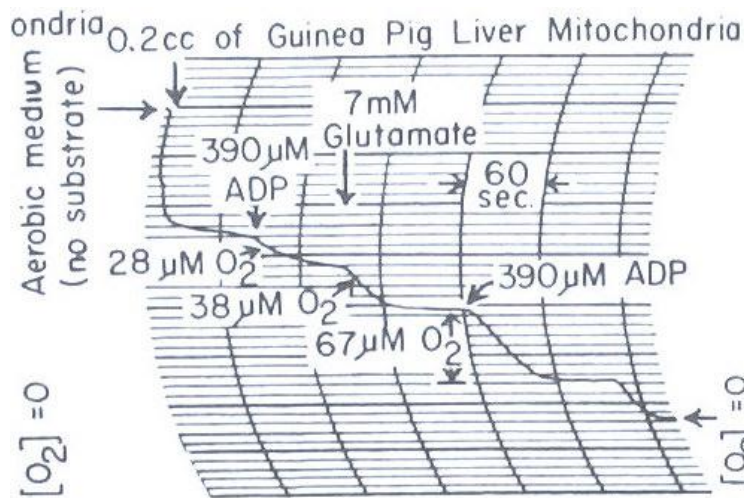


**Fig. 5.1. Respiratory states.** Coupling control in isolated mitochondria with glutamate as a substrate, to study the content of endogenous substrate (States 1 and 2), the ADP/O<sub>2</sub> ratio, and the respiratory control ratio (State 3/ State 4); zero oxygen calibration at State 5 (Chance and Williams 1955 I; Fig. 4B).

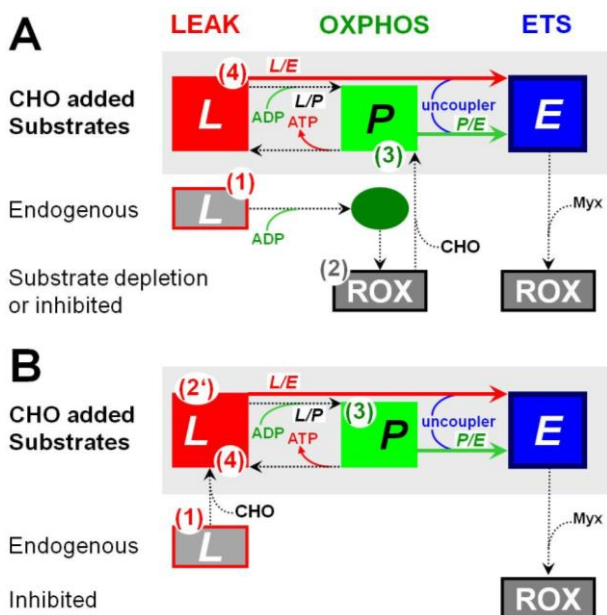


**Fig. 5.2. Coupling control.** Respiratory states (A) in the classical sequence from States 1 to 4 (numbers in parantheses) with addition of ADP to induce State 2 for measurement of residual oxygen consumption (ROX) followed by substrate addition (CHO) to initiate State 3, and (B) in an alternative protocol with initial addition of CHO substrates to induce a LEAK state in the absence of adenylates (L; 2'), followed by addition of saturating ADP to measure OXPHOS capacity, P (Gnaiger 2009).

The classical titration protocol (Fig. 5.1 and 5.2A) starts with addition of mitochondria to air-saturated isotonic medium with inorganic phosphate in State 1 (e<sub>N</sub>, endogenous substrates, no adenylates). Addition of ADP



induces a transient activation by ADP to effectively exhaust endogenous substrates, after which State 2 is a substrate-depleted state of residual oxygen consumption ( $+D_{ROX}$ ). ADP- and substrate activation is achieved in State 3 (high ADP, close to OXPHOS capacity,  $P$ ) by addition of substrate. In this state  $G_P$ , respiration is high and ADP is depleted by phosphorylation to ATP ( $\rightarrow T_L$ ). Respiration drops in the transition to State 4, which is an ADP-limited resting state in the presence of ATP ( $T$ , **LEAK state,  $L$** ). A second ADP titration ( $+D_P$ ) is followed by another State 3 $\rightarrow$ State 4 transition ( $D_P \rightarrow T_L$ ) at a higher final ATP concentration. Finally, respiration becomes oxygen limited after the aerobic-anoxic transition ( $\rightarrow$ anox) in the closed oxygraph chamber (State 5; Tab 5.1).

An alternative, conventional protocol (Fig. 5.2B) was introduced by Chance and Williams and is applied in many laboratories for measuring respiratory control ratios and ADP:O ratios (e.g. with succinate+rotenone; Fig. 4.5). The sequence of respiratory states is from State 1,  $e_N$  (endogenous substrates, no adenylates), to a LEAK state after addition of rotenone and succinate,  $S(Rot)_L$ , State 3 after addition of ADP ( $+D_P$ ), and another LEAK state or State 4 after phosphorylation of ADP to ATP ( $\rightarrow T_L$ ):



The original definition of State 2 (Tab. 5.1) is opposite to the state obtained in the absence of ADP but presence of substrate (Tab. 5.2).

**Table 5.1. Metabolic states of mitochondria (Chance and Williams, 1956; TABLE V).**

State	$[O_2]$	ADP level	Substrate level	Respiration rate	Rate-limiting substance	New abbreviation, example with $S(Rot)$	Coupling state
1	>0	Low	Low	Slow	ADP	$e_N$	
2	>0	High	~0	Slow	Substrate	$e_D$	ROX
3	>0	High	High	Fast	respiratory chain	$S(Rot)_{TD}$	OXPHOS
4	>0	Low	High	Slow	ADP	$S(Rot)_T$	LEAK
5	<0	High	High	0	Oxygen	$S(Rot)_{anox_T}$	

**Table 5.2. Definition of mitochondrial respiratory states. “Chance and Williams (1956) proposed a convention following the typical order of addition of agents during an experiment:” (Nicholls and Ferguson, 1992).**

		New abbreviation, example with $S(Rot)$	Coupling state
State 1:	mitochondria alone (in the presence of Pi)	$e_N$	
State 2:	substrate added, respiration low due to lack of ADP	$S(Rot)_N$	LEAK
State 3:	a limited amount of ADP added, allowing rapid respiration	$S(Rot)_D$ or $S(Rot)_{TD}$	OXPHOS
State 4:	All ADP converted to ATP, respiration slows	$S(Rot)_T$	LEAK
State 5:	Anoxia	$S(Rot)_{anox_T}$	

States 2 (Tab. 5.1) and  $L_N$  (Tab. 5.2) are functionally different states of ROX and LEAK respiration. ‘We have sought independent controls on whether State 2 corresponds to complete oxidation of the system. It is

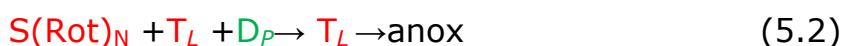


logical that this be so, for respiration is zero in State 2 because substrate, not phosphate acceptor, is limiting' (Chance and Williams 1955). In contrast, state  $L_N$  and State 4 ( $L_T$ ) are LEAK states, which yield significantly different oxygen kinetics of isolated mitochondria (Gnaiger et al 1998). The State 2 and 4 terminology has become confusing: '.. the controlled respiration prior to addition of ADP, which is strictly termed "state 2", is functionally the same as state 4, and the latter term is usually used for both states' (Nicholls and Ferguson 1992). Alchemy has a tradition of using the same term for multiple meanings and different terms for the same. A terminological extension from integers to the fraction  $3\frac{1}{2}$  has been suggested to indicate an intermediate mitochondrial energy state somewhere between States 3 and 4. Paradoxically, a fractional numbering system (real numbers of mathematics) would suggest that ADP-activated hypoxia were intermediate between States 3.0 and 5.0, i.e. State 4.0. This state of terminology requires fundamental reconsideration for clarification, particularly for extending bioenergetics to mitochondrial respiratory physiology and OXPHOS analysis.

## 2.1. LEAK Respiration, $L$

States  $S(\text{Rot})_N$  and  $S(\text{Rot})_T$  (State  $L_N$  and  $L_T$  or State 4) provide different states for estimating LEAK respiration. If ATPase activity causes any recycling of ATP to ADP, then some activation of respiration by phosphorylation occurs in state  $S(\text{Rot})_T$ . The aim is the induction of an  $L$  state for proper assessment of respiration merely compensating for LEAK (proton leak, electron slip and cation cycling in contrast to ATP synthase activity), in **nonphosphorylating respiration** of mitochondria in a partially coupled state. The increase of membrane potential must be considered in comparison to the ADP-stimulated OXPHOS state, hence determination of LEAK respiration may be considered as a maximum estimate.

The above protocol is varied in order to apply physiological high ATP concentrations (in the range of 1-5 mM; Gnaiger et al 2000; Gnaiger 2001),



When State 1 is not measured, the protocol starts with the LEAK state  $S(\text{Rot})_N$ . After addition of ATP ( $+T_L$ ), the system remains in a LEAK state; the ATPase effect is evaluated in the transition from  $S(\text{Rot})_N$  to  $S(\text{Rot})_T$  ( $+T_L$ , State 4; now the numerical sequence of states does not make sense).

## 2.2. OXPHOS Capacity, $P$

Stimulation by ADP ( $+D$ ) yields state  $S(\text{Rot})_{TD}$  for assessment of the capacity of oxidative phosphorylation (OXPHOS, state  $P$ ). The 'state TD' is different from the conventional State 3, due to the high ATP concentration, simulating physiological intracellular conditions. This





protocol requires careful isolation of mitochondria without ATPase activity, and therefore cannot be applied to permeabilized fibres or permeabilized cells. In general, ADP-saturated respiration in the presence of substrates yields the OXPHOS capacity,  $S(\text{Rot})_P$ . Mitochondria respiring at OXPHOS capacity generate a proton gradient by proton pumping (CI, CIII, CIV) which is partially utilized by the ATP synthase to drive phosphorylation (coupled respiration) and is partially dissipated due to proton leaks (uncoupled respiration). In the OXPHOS state, therefore, mitochondria are in a **partially coupled** (or loosely coupled) state.

### 2.3. Electron Transfer System Capacity, $E$

The capacity of the electron transfer system (ETS) is evaluated in an open-circuit operation of the transmembrane proton gradient. The open-circuit state is established experimentally by complete uncoupling (**noncoupled state**) using protonophores (uncouplers, such as FCCP or DNP) at optimum concentration for stimulation of maximum flux. ETS potentially exceeds the OXPHOS capacity. The important difference between ETS (state  $E$ ; noncoupled) and OXPHOS capacity (state  $P$ ; partially coupled) is somehow obscured when referring to the noncoupled state as State 3u (u for uncoupled).

OXPHOS and ETS capacity, as well as the difference between these states, depend on the types of substrates and substrate combinations applied in a respiratory protocol. Multiple substrate-uncoupler-inhibitor titration (SUIT) protocols are designed to evaluate the effects of substrate combinations on OXPHOS and ETS capacity.

$$GM_N + D_P + Omy_L + F_E + c + S_E + (\text{Rot})_E + (\text{MyX})_{\text{ROX}} \quad (5.3)$$

In protocol (5.3), two LEAK states,  $GM_L$ , are compared:  $GM_N$  and  $GM_{Omy}$ . See Appendix for abbreviations, such as glutamate and malate (G and M) and oligomycin (Omy). And substrate control is compared in coupling state  $E$ , in terms of noncoupled flux with CI, CI+II and CII substrates:  $GM_E$ ,  $GMS_E$  and  $S(\text{Rot})_E$ ; all in the noncoupled state supplemented with cytochrome c.

### 2.4. Respiratory States of the Intact Cell

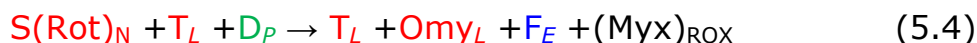
Cell respiration *in vivo* is regulated according to physiological activity, at intracellular non-saturating ADP levels in ROUTINE states of activity ( $R$ ), and increases under various conditions of activation. When incubated in culture medium, cells maintain a ROUTINE level of activity,  $C_R$  ( $C$ , intact cells;  $R$ , ROUTINE mitochondrial respiration; corrected for residual oxygen consumption due to oxidative side reactions). When incubated for short experimental periods in a medium devoid of organic substrates, the cells respire solely on endogenous substrates at the corresponding state of ROUTINE activity  $Ce_R$  ( $e$ , endogenous substrate supply).



ROUTINE cell respiration can be inhibited by oligomycin or (carboxy)atractyloside to a resting state, corresponding mainly to LEAK respiration ( $L$ ), comparable to isolated mitochondria but without disturbing intracellular substrate conditions by cell membrane permeabilization (Fig. 1.2). It is difficult to stimulate intact cells to maximum OXPHOS activity, whereas uncouplers of OXPHOS are cell membrane permeable, and cells with standard or endogenous substrate supply can be activated by uncoupling to reveal the ETS capacity (state  $E$ ). Coupling control ratios, therefore, can be studied in cells with intact plasma membranes.

### 3. Coupling Control Ratios (CCR), Respiratory Control Ratio (RCR), Uncoupling Control Ratio (UCR)

Consider the following protocol in isolated mitochondria:



where the example discussed above (protocol 5.2) is extended by addition of oligomycin (+Omy), titration of uncoupler (+F) and inhibitor myxothiazol (+Myx). The respiratory adenylate control ratio, RCR, is conventionally defined as the ADP-activated flux to measure coupled OXPHOS capacity ( $P$ ; State 3) divided by LEAK flux ( $L$ ; no adenylates, or State 4, or oligomycin-inhibited). An important aim in respirometric assays is the evaluation of the state of coupling or uncoupling. Unrelated to uncoupling, OXPHOS capacity and hence the RCR are lowered if a low capacity of the phosphorylation system limits OXPHOS capacity. This is the case when noncoupled flux as a measure of ETS capacity ( $E$ ) is higher than coupled flux ( $P$ ) and there is an apparent ETS excess capacity over OXPHOS capacity. The reference state appropriate for defining an index of coupling, therefore, is not coupled OXPHOS capacity ( $P$ ) but the state yielding noncoupled electron transfer capacity ( $E$ ). The RCR has the mathematically inconvenient property of increasing to infinity from a minimum of 1.0. In contrast, coupling control ratios (CCR) are defined between limits of 0.0 and 1.0, as derived from flux control analysis. Coupling control ratios are flux control ratios at constant substrate supply (Gnaiger 2009). The CCR expressing the 'leakiness' of mitochondria in the partially coupled state, is the **LEAK control ratio**,  $L/E$ ,

$$L/E = S(\text{Rot})_L / S(\text{Rot})_E \quad (5.5)$$

(using the same abbreviation for a metabolic state and for oxygen flux in this metabolic state).

In the absence of ATPase activity, LEAK flux is equal in states  $S(\text{Rot})_N$ ,  $S(\text{Rot})_T$  and  $S(\text{Rot})_{\text{omy}}$ , all providing an estimate of LEAK respiration,  $S(\text{Rot})_L$ . The LEAK control ratio,  $L/E$ , can be measured in intact cells,

$$L/E = C_L / C_E \quad (5.6)$$



If ATPase activity is responsible for  $S(\text{Rot})_T > S(\text{Rot})_{\text{omy}}$ , the increased  $S(\text{Rot})_T$  increases the apparent  $L/E$  ratio, and  $S(\text{Rot})_{\text{omy}}$  provides a more accurate estimate of LEAK.  $C_L$  and  $C_E$  are LEAK respiration and ETS capacity measured in coupled oligomycin-inhibited and noncoupled cells, corrected for residual oxygen consumption.

In cells, the **ROUTINE control ratio**,  $R/E$ , is,

$$R/E = C_R / C_E \quad (5.7)$$

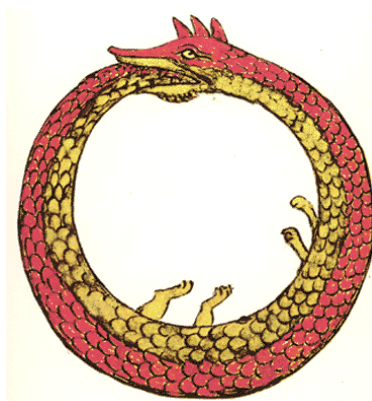
where  $C_R$  is ROUTINE respiration, which is partially coupled and reflects the state of activation of cellular respiration according to routine ATP demand and degree of coupling. The (inverse)  $UCR_{E/R}$  is an expression of the capacity of the electron transfer system relative to ROUTINE respiration.

Analogous to the ROUTINE control ratio in cells, the **phosphorylation system control ratio**,  $P/E$ , relates OXPHOS capacity ( $P$ ; State 3 at saturating [ADP]) to noncoupled respiration. In the present example, the OXPHOS/ETS control ratio,  $P/E = UCR_{E/P}^{-1}$  is,

$$P/E = S(\text{Rot})_P / S(\text{Rot})_E \quad (5.8)$$

The  $P/E$  control ratio is an expression of how close the capacity of partially coupled oxidative phosphorylation ( $P$ ) approaches the capacity for noncoupled electron transfer ( $E$ ). If  $P/E < 1.0$ , then the phosphorylation system exerts control over OXPHOS capacity.

Comparable to ROUTINE respiration in intact cells, various intermediary ADP controlled states,  $S(\text{Rot})_{T[\text{ADP}]}$ , can be established in isolated mitochondria by varying ADP supply over a wide range (Gnaiger et al 2000). Corresponding steady-state ADP concentrations regulate respiratory flux at graded levels between the minimum of LEAK flux and the maximum of OXPHOS capacity. OXPHOS capacity at state TD can be calculated as  $J_{\text{max}}$  from hyperbolic ADP kinetics, or directly measured at saturating ADP concentration.





## Chapter 6. Conversions of Metabolic Fluxes

### 1. Temperature Adjustment of Flux

Manometric techniques (Warburg apparatus) require good temperature control and were used extensively at 37 °C for respirometry with mammalian cells up to the middle of the last century, and later occasionally with isolated mitochondria. Spectrophotometers and Clark-type oxygraphs had comparatively poor or no temperature control and thus measurements were performed at room temperature (Chance and Williams 1955). This conceptually trivial (technically less simple) reason is largely forgotten but a convention is continued, and frequently mammalian mitochondrial respiration is still measured at 25 °C or 30 °C in 'modern' bioenergetics. Mitochondrial physiology requires functional measurements at physiological temperature. A  $Q_{10}$  of 2 (multiplication factor for an increase by 10 °C) is frequently assumed for adjustment to physiological temperature, but can be considered as an approximation only.

Metabolic reactions are not a linear function of temperature.  $Q_{10} = 2$  (Eq. 6.1a) is an approximation for the temperature dependence of chemical reactions in general (Arrhenius equation) and metabolic fluxes in particular. To adjust flux,  $J_1$ , measured at temperature  $T_1$  (for instance,  $T_1=25$  °C; Tab. 6.1) to the physiological temperature,  $T_2=37$  °C, the exponential relation (Eq. 6.1) is used to calculate  $J_2$  (37 °C),

$$J_2 = 10^{\log J_1 - \log Q_{10} \cdot \left(\frac{10}{T_1 - T_2}\right)} \quad (6.1)$$

The derivation is obtained from the definition of the  $Q_{10}$ ,

$$Q_{10} = \left(\frac{J_1}{J_2}\right)^{\frac{10}{T_1 - T_2}} \quad (6.1a)$$

In log transformation, Eq. 6.1a is,

$$\log Q_{10} = (\log J_1 - \log J_2) \cdot \left(\frac{10}{T_1 - T_2}\right) \quad (6.1b)$$

Division by the term  $10/(T_1 - T_2)$  yields,

$$\log Q_{10} / \left(\frac{10}{T_1 - T_2}\right) = \log J_1 - \log J_2 \quad (6.1c)$$



and solving for  $\log J_2$ ,

$$\log J_2 = \log J_1 - \log Q_{10} / \left( \frac{10}{T_1 - T_2} \right) \quad (6.1d)$$

Eq. 6.1 is then obtained by inserting Eq. 6.1d into Eq. 6.1e,

$$J_2 = 10^{\log J_2} \quad (6.1e)$$

For any given  $Q_{10}$  and temperature difference  $\Delta T = T_1 - T_2$ , a multiplication factor  $F_{\Delta T}$  can be calculated from Eq. 6.1 to obtain  $J_2$  (Tab. 6.1),

$$J_2 = J_1 \cdot F_{\Delta T} \quad (6.2a)$$

$$F_{\Delta T} = 10^{-\log Q_{10} / \left( \frac{10}{T_1 - T_2} \right)} \quad (6.2b)$$

The  $Q_{10}$  is the  $F_{\Delta T}$  (Eq. 6.2b) for a temperature difference of 10 °C. Obviously, if  $T_2$  is 37 °C and  $T_1$  is 27 °C ( $T_1 - T_2 = -10$ ), then the exponent in Eq. 6.2b is  $\log Q_{10}$ , and  $F_{\Delta T} = Q_{10}$ . For  $T_1$  of 25 °C or 30 °C and  $Q_{10} = 2$ , the  $\Delta T$ -factor  $F_{\Delta T}$  is 2.30 and 1.62, respectively. Clearly, if respiratory flux at physiological temperature is of interest, respiration should be measured at this temperature rather than adjusted on the basis of potentially inaccurate assumptions about the  $Q_{10}$ .

**Tab. 6.1.** Conversion of metabolic flux from experimental temperature  $T_1$  to adjusted temperature  $T_2$ , based on  $Q_{10}$  values of 2.0, 1.8 and 2.2.

<b><math>Q_{10}</math></b>	<b>2.00</b>			<b>1.80</b>			<b>2.20</b>		
$T_1$ °C	25	30	37	25	30	37	25	30	37
$T_2$ °C	$F_{\Delta T}$	$F_{\Delta T}$	$F_{\Delta T}$	$F_{\Delta T}$	$F_{\Delta T}$	$F_{\Delta T}$	$F_{\Delta T}$	$F_{\Delta T}$	$F_{\Delta T}$
25	1.00	0.71	0.44	1.00	0.75	0.49	1.00	0.67	0.39
30	1.41	1.00	0.62	1.34	1.00	0.66	1.48	1.00	0.58
35	2.00	1.41	0.87	1.80	1.34	0.89	2.20	1.48	0.85
37	2.30	1.62	1.00	2.02	1.51	1.00	2.58	1.74	1.00
38	2.46	1.74	1.07	2.15	1.60	1.06	2.79	1.88	1.08
39	2.64	1.87	1.15	2.28	1.70	1.12	3.02	2.03	1.17
40	2.83	2.00	1.23	2.41	1.80	1.19	3.26	2.20	1.27





## 2. Conversion Factors for Units of Oxygen Flux

Comparability of quantitative results on respiratory fluxes is aided by using common units. Considering the variety of units used in various disciplines of respiratory physiology, a common basis may only be found with reference to proper *SI* units (Gnaiger 1983, 1993).

When respiratory activity is expressed per volume of the Oxygraph chamber or volume-specific oxygen flux, the base *SI* unit is  $[\text{mol}\cdot\text{s}^{-1}\cdot\text{m}^{-3}]$ . Since oxygen concentration in pure water at equilibrium with air at standard barometric pressure of 100 kPa is 254.8 to 207.3  $\mu\text{mol}\cdot\text{dm}^{-3}$  (25 to 37 °C), it is most practical to express oxygen concentration in  $\mu\text{M}$  units,

$$1 \mu\text{mol O}_2/\text{litre} = 1 \mu\text{mol}/\text{dm}^3 = 1 \mu\text{M} = 1 \text{ nmol}/\text{ml} = 1 \text{ nmol}/\text{cm}^3$$

**Table A3.1. Conversion of various units into *SI* units** when expressing respiration as mass-specific oxygen flux.

$J$	[Unit <sub><i>j</i></sub> ]	x	Factor	=	$J_{\text{O}_2}$ [ <i>SI</i> -Unit]
					$\text{nmol O}_2\cdot\text{s}^{-1}\cdot\text{g}^{-1}$
					$\text{pmol O}_2\cdot\text{s}^{-1}\cdot\text{mg}^{-1}$
12	$\text{ng}\cdot\text{atom O}\cdot\text{min}^{-1}\cdot\text{mg}^{-1}$	x	8.33	=	100
12	$\mu\text{mol O}\cdot\text{min}^{-1}\cdot\text{g}^{-1}$	x	8.33	=	100
12,000	$\text{natom O}\cdot\text{min}^{-1}\cdot\text{g}^{-1}$	x	0.00833	=	100
6	$\text{nmol O}_2\cdot\text{min}^{-1}\cdot\text{mg}^{-1}$	x	16.67	=	100
6	$\mu\text{mol O}_2\cdot\text{min}^{-1}\cdot\text{g}^{-1}$	x	16.67	=	100
6	$\text{mmol O}_2\cdot\text{min}^{-1}\cdot\text{kg}^{-1}$	x	16.67	=	100

The proper *SI* unit,  $\mu\text{mol O}_2\cdot\text{s}^{-1}\cdot\text{dm}^{-3}$ , is used for the corresponding respiratory flux in the classical bioenergetic literature (Chance and Williams 1956). In the bioenergetic context of  $\text{H}^+/2\text{e}$  or  $\text{H}^+/\text{O}$  ratios (Mitchell and Moyle 1967) or P:O ratios, corresponding fluxes were then frequently expressed as  $J_P/J_O$ , where  $J_{\text{O}_2} = 2\cdot J_O$ , the latter in 'bioenergetic' units  $[\text{natoms O}\cdot\text{s}^{-1}\cdot\text{ml}^{-1}]$  (Slater et al 1973). In bioenergetics a variety of expressions is used for units of amount of oxygen (natoms oxygen; natoms O;  $\text{ng}\cdot\text{atom O}$ ;  $\text{nmol O}$ ), with the identical meaning: 0.5  $\text{nmol O}_2$ .

## 3. Fundamental Constants and Conversion Factors

Boltzmann constant	$k$	$1.3807\cdot 10^{-23} \text{ J}\cdot\text{K}^{-1}$
Gas constant	$R$	$8.314510 \text{ J}\cdot\text{mol}^{-1}\cdot\text{K}^{-1}$
Avogadro constant	$N_A$	$6.02214\cdot 10^{23} \text{ mol}^{-1}$
Elementary charge	$e$	$1.602177\cdot 10^{-19} \text{ C}$
Farady constant	$F=eN_A$	$96,485.3 \text{ C}\cdot\text{mol}^{-1}$ ( $96.4853 \text{ kJ}\cdot\text{mol}^{-1}/\text{V}$ )
Absolute temperature	$T$	273.15; 298.15; 310.15 K at 0; 25; 37 °C
$RT$		2.271; 2.479; 2.579 $\text{kJ}\cdot\text{mol}^{-1}$ at 0; 25; 37 °C
$\ln(10)$		2.3026
$RT\cdot\ln(10)$		5.229; 5.708; 5.938 $\text{kJ}\cdot\text{mol}^{-1}$ at 0; 25; 37 °C
$(RT/F)\cdot\ln(10)$		54.20; 59.16; 61.54 mV at 0; 25; 37 °C
$1/4F$		2.591 $\mu\text{mol}/(4 \text{ C})$



## Appendix: Abbreviations

A1. Respiratory Coupling States .....	54
A2. Substrates, Uncouplers and Inhibitors .....	56

### A1. Respiratory Coupling States and Coupling Control Ratios

Mitochondrial respiratory states and coupling control ratios are defined in isolated mitochondria or permeabilized cells and tissues, at a given substrate (and inhibitor) combination (X), and in intact cells (C). In a medium without energy substrates, cells respire on endogenous substrate ( $C_e$ ), whereas culture medium or medium of varied composition  $m$  provides substrates for respiration and growth ( $C_m$ ). Isolated mitochondria (Imt) are distinguished from intact cells (C), permeabilized cells (PC) or permeabilized tissue (PT).

#### Coupling control states

$E$	Electron transfer system capacity state
$L$	LEAK state
$P$	OXPHOS capacity state
$R$	ROUTINE state of cell respiration

#### Coupling control ratios (CCR)

$L/E$	LEAK CCR
$P/E$	Phosphorylation system CCR
$R/E$	ROUTINE CCR

#### A1.1. Residual Oxygen Consumption - ROX

$Imt_{ROX}$	Oxygen uptake due to residual oxidative side reactions in isolated mitochondria, estimated by inhibiting various respiratory complexes after uncoupling, is used to correct mitochondrial respiratory states. Correction is controversial due to the possible induction of electron leak from the electron transfer system by application of specific inhibitors.
$PC_{ROX}$	or $PT_{ROX}$ , probably higher than $Imt_{ROX}$ , where isolation eliminates organelles and non-mitochondrial membranes with oxygen-consuming activity.
$C_{ROX}$	Residual oxygen consumption in intact cells, higher than $PC_{ROX}$ , where permeabilization eliminates specific substrates for ROX.

#### A1.2. ETS Capacity - State $E$

$X_E$	= $X_E' - Imt_{ROX}$ (in Imt; $X_E' - PC_{ROX}$ in PC); ETS capacity (noncoupled respiration) in the presence of substrate X.
$C_E$	= $C_E' - C_{ROX}$ ; noncoupled respiration, measure of ETS capacity at optimum uncoupler concentration. Apparent ETS



capacity,  $C_E'$  (noncoupled respiration, not corrected for  $C_{ROX}$ ). Level flow in the terminology of thermodynamics of irreversible processes.

$ROX/E'$  =  $C_{ROX}/C_E'$ ; flux control ratio of oxidative side-reactions, normalized for total uncoupled respiratory flux.

### A.1.3. OXPHOS Capacity – State P

$X_P$  OXPHOS capacity, measured after activation by saturating ADP concentration.  $X_P$  may be estimated in the coupled states  $X_D$  or  $X_{TD}$  (State 3), corrected for ROX.

$P/E$  =  $X_P/X_E$ ; OXPHOS control ratio, measures how close  $X_P$  approaches the upper limit of ETS capacity,  $X_E$ . Excess ETS capacity over the phosphorylation system yields  $P/E < 1.0$ ; weak coupling reduces the effect of ETS excess capacity and increases respiration ( $X_P$ ) without increasing phosphorylation.

### A.1.4. ROUTINE Respiration – State R

$C_R$  =  $C_R' - C_{ROX}$ ; ROUTINE respiration (ROX-corrected).

$R/E$  =  $C_R/C_E$ ; ROUTINE control ratio, measures how close ROUTINE activity of cells approaches the upper limit of  $C_E$ .

### A1.5. LEAK Respiration – State L

$X_L$  =  $X_L' - X_{ROX}$ ; LEAK respiration, in the partially coupled state after eliminating phosphorylation, e.g. after depletion of ADP in the presence or absence of ATP (N or T), or after inhibiting ANT (Cat, Atr) or ATP synthase (Omy). Static head in thermodynamics of irreversible processes.

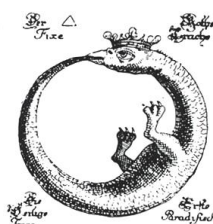
$C_L$  LEAK respiration in the cell, measured after inhibiting the ANT (Cat, Atr) or ATP synthase (Omy).

$L/E$  =  $C_L/C_E$  (or  $X_L/X_E$ ); LEAK control ratio, measures how close  $C_L$  or  $X_L$  approaches the upper limit of  $C_E$  or  $X_E$ , which is reached in noncoupled mitochondria ( $L/E = 1.0$ ).

net $R/E$  =  $(R-L)/E$ ; net ROUTINE control ratio; fraction of ETS capacity directly utilized to drive phosphorylation of ADP to ATP.



<http://www.bioblast.at/index.php/MitoPedia> Glossary: Respiratory states







## A2. Substrates, Uncouplers and Inhibitors

### A2.1. Oxygraph-2k Manual Titrations: Mitochondria, Homogenate, Permeabilized Cells and Tissues



**Tab. A2.1.** O2k manual titrations for a chamber volume of 2.0 ml

Substrates	Event	Concentration in syringe (solvent)	Storage [°C]	Final conc. in 2 ml O2k-chamber	Titration [μl] into 2 ml	Syringe [μl]
Pyruvate	P	2 M (H <sub>2</sub> O)	fresh	5 mM	5	25
Malate	M	0.8 M (H <sub>2</sub> O)	-20	2 mM	5	25
Glutamate	G	2 M (H <sub>2</sub> O)	-20	10 mM	10	25
Succinate	S	1 M (H <sub>2</sub> O)	-20	10 mM	20	50
Ascorbate	As	0.8 M (H <sub>2</sub> O)	-20	2 mM	5	25
TMPD	Tm	0.2 M (H <sub>2</sub> O)	-20	0.5 mM	5	25
Cyt. C	c	4 mM (H <sub>2</sub> O)	-20	10 μM	5	25
ADP+ Mg <sup>2+</sup>	D	0.5 M (H <sub>2</sub> O)	-80	1 - 5 mM	4 - 20	10
ATP+ Mg <sup>2+</sup>	T	0.5 M (H <sub>2</sub> O)	-80	1 - 5 mM	4 - 20	10
<b>Uncoupler</b>						
FCCP <sup>1</sup>	F	1 mM (EtOH)	-20	0.5 μM steps	1 μl steps	10
FCCP-MiR06	F	0.1 mM (EtOH)	-20	0.05 μM steps	1 μl steps	10
<b>Inhibitors</b>						
Rotenone	Rot	1.0 or 0.2 mM (EtOH)	-20	0.5 or 0.1 μM	1	10
Malonic acid	Mna	2 M (H <sub>2</sub> O)	fresh	5 mM	5	25
Antimycin A	Ama	5 mM (EtOH)	-20	2.5 μM	1	10
Myxothiazol	Myx	1 mM (EtOH)	-20	0.5 μM	1	10
Sodium azide	Azd	4 M (H <sub>2</sub> O)	-20	≥100 mM	≥50	50
KCN	Kcn	1 M (H <sub>2</sub> O)	fresh	1.0 mM	2	10
Oligomycin	Omy	4 mg/ml (EtOH)	-20	2 μg/ml	1	10
Atractyloside	Atr	50 mM (H <sub>2</sub> O)	-20	0.75 mM	30	50
<b>Cell perm.</b>						
Digitonin	Dig	10 mg/ml (DMSO)	-20	10 μg · 10 <sup>-6</sup> cells	1 μl 10 <sup>-6</sup> cells	10
<b>Other</b>						
Catalase	Ctl	112,000 IU/ml (MiR05)	-20	280 IU/ml	5	25
Ionomycin	lmy	0.5 mg/ml (EtOH)	-20	0.5 μg/ml	2	10

<sup>1</sup>Higher FCCP concentration: in various culture media (e.g. RPMI, DMEM) and for TIP2k.



[http://www.orooboros.at/?Protocols\\_titrations](http://www.orooboros.at/?Protocols_titrations)



## A2.2. Substrates of the TCA cycle and major entries

Single capital letters for the most commonly used substrates

P	Pyruvate
G	Glutamate
M	Malate
S	Succinate
F	Fumarate
Og	Oxoglutarate
Ce	Cellular substrates <i>in vivo</i> , endogenous
Cm	Cellular substrates <i>in vivo</i> , with exogenous substrate supply from culture medium or serum

## A2.3. Other substrates and redox components of the respiratory system

Oca	Octanoate
Paa	Palmitate
Oct	Octanoyl carnitine
Pal	Palmitoyl carnitine
As	Ascorbate
Tm	TMPD
c	Cytochrome c
Gp	Glycerophosphate

## A2.4. Phosphorylation system

Adenylates,  $P_i$ , uncouplers, downstream inhibitors of ATP synthase, ANT, or phosphate are denoted by subscripts. If  $P_i$  is always present at saturating concentration, it does not have to be indicated in the titration protocols.

$P_i$	Inorganic phosphate
N	no adenylates added (state $L$ )
D	ADP at saturating concentration (state $P$ : saturating [ADP])
D0.2	ADP at specified concentration (saturating versus non-saturating ADP is frequently not specified in State 3)
T	ATP (state $L_T$ )
TD	ATP+ADP (state $P$ , in the presence of physiological high (mM) ATP concentrations)
T[ADP]	High ATP and varying ADP concentrations, in the range between states T and TD.
u	Uncoupler at optimum concentration for maximum noncoupled flux (state $E$ ).



[http://www.bioblast.at/index.php/List\\_of\\_substrates\\_and\\_metabolites](http://www.bioblast.at/index.php/List_of_substrates_and_metabolites)



[http://www.bioblast.at/index.php/List\\_of\\_uncouplers](http://www.bioblast.at/index.php/List_of_uncouplers)



## A2.5. Inhibitors of respiratory complexes, dehydrogenases or transporters

Atr	Atractyloside (state $L_{Atr}$ )
Ama	Antimycin A
Azd	Sodium azide
Hci	Hydroxycinnamate
Kcn	KCN
Mna	Malonate
Myx	Myxothiazol
Omy	Oligomycin (state $L_{Omy}$ )
Rot	Rotenone



[http://www.bioblast.at/index.php/List\\_of\\_inhibitors](http://www.bioblast.at/index.php/List_of_inhibitors)

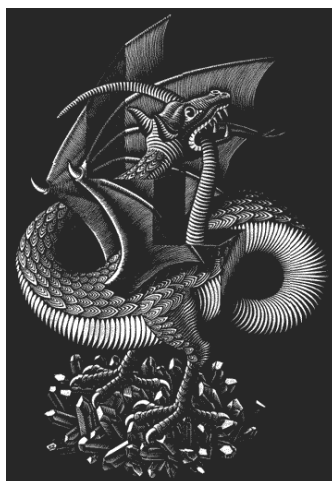
## A2.6. Protocols

Letters in normal font are used for the substrates X.

Subscripts are used for effectors of the phosphorylation system and for indicating coupling control states.

Example: In the protocol  $*:PM_N + D + c + G + S + F + (Rot) + (Myx+..)$ , the respiratory state after addition of rotenone is:  $PMGSc(Rot)_E$ . With reference to this protocol, it may be convenient to use an abbreviation, such as  $S(Rot)_E$ , e.g. if cytochrome c addition is used as a quality control and exerts no effect on respiratory capacity.

\*Suspended cells may be permeabilized in the oxygraph chamber with digitonin (Dig), after measurement of endogenous respiration in mitochondrial respiration medium. The initial protocol is indicated above as \*; referring to the initial steps of endogenous respiration and permeabilization:  $Ce_R + PM + Dig$ .



Oroboros by M.C. Escher



## References

Open Access to the full list of references and notes:



[http://www.bioblast.at/index.php/Gnaiger\\_2012\\_MitoPathways](http://www.bioblast.at/index.php/Gnaiger_2012_MitoPathways)

Selected references (mainly sources of figures, tables, and basic concepts):

- Boushel R, Gnaiger E, Schjerling P, Skovbro M, Kraunsoe R, Flemming D (2007) Patients with Type 2 Diabetes have normal mitochondrial function in skeletal muscle. *Diabetologia* 50: 790-796.
- Chance B, Williams GR (1955) Respiratory enzymes in oxidative phosphorylation. I. Kinetics of oxygen utilization. *J Biol Chem* 217: 383-393.
- Chance B, Williams GR (1955) Respiratory enzymes in oxidative phosphorylation. III. The steady state. *J Biol Chem* 217: 409-427.
- Gnaiger E (1993) Nonequilibrium thermodynamics of energy transformations. *Pure Appl Chem* 65: 1983-2002.
- Gnaiger E (1993) Efficiency and power strategies under hypoxia. Is low efficiency at high glycolytic ATP production a paradox? In: *Surviving Hypoxia: Mechanisms of Control and Adaptation*. Hochachka PW, Lutz PL, Sick T, Rosenthal M, Van den Thillart G (eds) CRC Press, Boca Raton, Ann Arbor, London, Tokyo: 77-109.
- Gnaiger E, Méndez G, Hand SC (2000) High phosphorylation efficiency and depression of uncoupled respiration in mitochondria under hypoxia. *Proc Natl Acad Sci U S A* 97: 11080-11085.
- Gnaiger E (2008) Polarographic oxygen sensors, the oxygraph and high-resolution respirometry to assess mitochondrial function. In: *Mitochondrial Dysfunction in Drug-Induced Toxicity* (Dykens JA, Will Y, eds) John Wiley: 327-352.
- Gnaiger E (2009) Capacity of oxidative phosphorylation in human skeletal muscle. New perspectives of mitochondrial physiology. *Int J Biochem Cell Biol* 41: 1837-1845.
- Gutman M, Coles CJ, Singer TP, Casida JE (1971) On the functional organization of the respiratory chain at the dehydrogenase-coenzyme Q junction. *Biochemistry* 10: 2036-2043.
- Harris EJ, Manger JR (1969) Intersubstrate competitions and evidence for compartmentation in mitochondria. *Biochem J* 113: 617-628.
- Hatefi Y, Haavik AG, Fowler LR, Griffiths DE (1962) Studies on the electron transfer system. XLII. Reconstitution of the electron transfer system. *J Biol Chem* 237: 2661-2669.
- Jacobs RA, Boushel R, Wright-Paradis C, Calbet JA, Robach P, Gnaiger E, Lundby C (2012) Mitochondrial function in human skeletal muscle following high altitude exposure. *Exp Physiol*. 2012 May 25. [Epub ahead of print]
- LaNoue KF, Schoolwerth AC (1979) Metabolite transport in mitochondria. *Annu Rev Biochem* 48: 871-922
- LaNoue KF, Walajtys EI, Williamson JR (1973) Regulation of glutamate metabolism and interactions with the citric acid cycle in rat heart mitochondria. *J Biol Chem* 248: 7171-7183.
- Lemieux H, Semsroth S, Antretter H, Hoefler D, Gnaiger E (2011) Mitochondrial respiratory control and early defects of oxidative phosphorylation in the failing human heart. *Int J Biochem Cell Biol* 43: 1729-1738.



- Mitchell P, Moyle J (1967) Respiration-driven proton translocation in rat liver mitochondria. *Biochem J* 105: 1147-1162.
- Nicholls DG, Ferguson SJ (2002) *Bioenergetics 3*, Academic Press, London. 287 pp.
- Pesta D, Gnaiger E (2012) High-resolution respirometry. OXPHOS protocols for human cells and permeabilized fibres from small biopsies of human muscle. *Methods Mol Biol* 810: 25-58.
- Pesta D, Hoppel F, Macek C, Messner H, Faulhaber M, Kobel C, Parson W, Burtscher M, Schocke M, Gnaiger E (2011) Similar qualitative and quantitative changes of mitochondrial respiration following strength and endurance training in normoxia and hypoxia in sedentary humans. *Am J Physiol Regul Integr Comp Physiol* 301: R1078-R1087.
- Puchowicz MA, Varnes ME, Cohen BH, Friedman NR, Kerr DS, Hoppel CL (2004) Oxidative phosphorylation analysis: assessing the integrated functional activity of human skeletal muscle mitochondria - case studies. *Mitochondrion* 4: 377-385.
- Rasmussen HN, Rasmussen UF (1997) Small scale preparation of skeletal muscle mitochondria, criteria for integrity, and assays with reference to tissue function. *Mol Cell Biochem* 174: 55-60.
- Rasmussen UF, Rasmussen HN (2000) Human quadriceps muscle mitochondria: A functional characterization. *Mol Cell Biochem* 208: 37-44.
- Renner K, Amberger A, Konwalinka G, Gnaiger E (2003) Changes of mitochondrial respiration, mitochondrial content and cell size after induction of apoptosis in leukemia cells. *Biochim Biophys Acta* 1642: 115-123.
- Sjoevall F, Morota S, Hansson MJ, Friberg H, Gnaiger E, Elmer E (2010) Temporal increase of platelet mitochondrial respiration is negatively associated with clinical outcome in patients with sepsis. *Critical Care* 14: R214 doi:10.1186/cc9337
- Torres NV, Mateo F, Sicilia J, Meléndez-Hevia E (1988) Distribution of the flux control in convergent metabolic pathways: theory and application to experimental and simulated systems. *Int J Biochem* 20: 161-165.
- Votion DM, Gnaiger E, Lemieux H, Mouithys-Mickalad A, SerTEYN D (2012) Physical fitness and mitochondrial respiratory capacity in horse skeletal muscle. *PLoS One* 7: e34890.



Winfried Platzgummer - Oroboros in Thermodynamics (2010)



# Bioblast Wiki

Integrating the spirit of  
Gentle Science and  
Scientific Social  
Responsibility



OROBOROS O2k-Team<sup>1</sup>

**Bioblast** was launched as a glossary and index for high-resolution respirometry (OROBOROS INSTRUMENTS: **OroboPedia**) and Mitochondrial Physiology (**MitoPedia**), to find topics quickly, as a dynamic tool for summarizing definitions of terms, symbols and abbreviations - an innovative, collaborative wiki database, perhaps aiding the formation of a [Global Mitochondrial Network](#) [2,3].

**What is the aim?** Bioblast provides a platform for **Gentle Science** [4] in the spirit of Scientific Social Responsibility. Catalytically working as an *Information synthase* (see logo [3]), **MitoPedia** supports the decentralized evolution of a glossary of scientific terms, for developing a consistent nomenclature in the growing field of mitochondrial physiology. The corresponding category **Publications** provides a portal for sharing, disseminating and commenting relevant literature in mitochondrial physiology, with context-related 'filters' for references. Bioblast allows the *evolution* of a scientific publication - providing space for open discussions and extensions of an otherwise static *paper*. This applies specifically to the sections of *Methods and Materials*, *Discussion*, and *References*, which may be limited by space in original publications. Detailed information added and edited should be helpful in practice. For example, **O2k-Protocols** are found now more quickly and users are encouraged to contribute and share their expertise.

**How to register?** Write to us, and we will register you with your real name, as in a scientific publication. Anonymous or pseudonymous contributions to Bioblast do not follow the scientific attitude of publication. Mail to [barbara.meissner@oroboros.at](mailto:barbara.meissner@oroboros.at) for registration or if you need help in editing.

**How does it work?** We invite scientists, students, and technicians in mitochondrial physiology and pathology to join as 'active users' in the spirit of Gentle Science, to ensure that the Bioblast Wiki will develop into a database of top-quality scientific information. This can be achieved only by an expert-moderated wiki - with input and feedback of a large benevolent user community of experts in mitochondrial physiology.

All of you can shape the Bioblast Wiki by bringing together scientists working in divergent disciplines, to discuss, to resolve differences, to spread new knowledge and techniques; thus meeting the demand to integrate current developments in the methodologically and conceptually complex field of mitochondrial physiology.

1. Barbara Meissner, Anita Wiethüchter, Mario Fasching, Erich Gnaiger
2. A *wiki* (Hawaiian, meaning 'fast') is a dynamic and collaborative website. Cunningham Ward: [What is a Wiki](#); WikiWikiWeb: <http://www.wiki.org/wiki.cgi?WhatIsWiki> 2010-09-09
3. The **Bioblast logo** combines mitochondrial art, from '*ATP synthase congregation*' by Odra Noel, with the Oroboros, "the tail-eater" - a dragon forming a circle, where '*creation and the created become one in an inseparable process*' <http://www.mipart.at/index.php?oroboros-archetypical-symbol> 2010-11-29
4. Gentle Science Shapes the World - [http://www.bioblast.at/index.php/Gentle\\_Science](http://www.bioblast.at/index.php/Gentle_Science) 2012-11-29



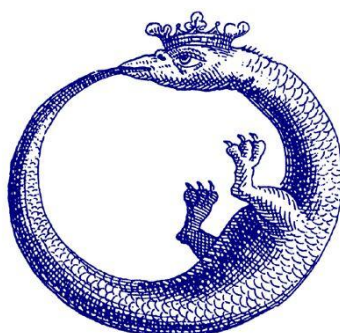
The Oroboros – the open door to OROBOROS INSTRUMENTS and the *MiPart* Gallery. Steel sculpture by Harald Kirchebner (2008). Foto by Philipp Gradl.



## THE OROBOROS

### FEEDING ON NEGATIVE ENTROPY?

The dragon forming a cycle, feeding on its own tail - in alchemy, the Oroboros is an emblem of the eternal, cyclic nature of the universe, combining idea and action, efficiency and power. The Oroboros is grasping the whole by the conception of the opposite, the divine process of creation and the evil backlash of destruction. In thermodynamics, the alchemist's search for the eternal Unity has been continued in the many efforts to construct a machine operating at 100% efficiency, the



Perpetuum Mobile. 100% efficiency is the prerequisite for a truly cyclic nature of energy flux through the biosphere. The notion of the arrow of time, introduced by the Second Law of thermodynamics, replaces the quest for 100% efficiency by the pursuit of a balanced management of the resources of energy and time. Such optimization of efficient material recycling and balanced resource utilization is a vital responsibility of modern society for the protection of local and global ecological systems.

The Oroboros is one of the rare universal examples where feeding on external negative entropy,  $d_e S/dt$ , is not true, as shown by the feedback loop and the system boundaries. In terms of ergodynamics, at any rate, Oroboros is the fine state of *non-thermodynamic equilibrium*.

Graphic from: Abraham Eleazar (1760)  
Uraltes chymisches Werk. 2nd ed, Leipzig

From: *What is Controlling Life? 50 years after Erwin Schrödinger's 'What is Life?'*  
(Gnaiger E, Gellerich FN, Wyss M, eds), *Modern Trends in BioThermoKinetics 3*  
Innsbruck Univ Press (1994): 316.





# A taste of Gentle Science **Bioblast**



[www.bioblast.at](http://www.bioblast.at)

[www.orooboros.at](http://www.orooboros.at)